

|safaa

| s a f a a □
Nn

ط...ٹ € ٹ...ہ € ٹ...ا € ٹ...ا € ٹ...ا € ٹ...د € ٹ...H € ٹ...@
...ى €

4.1 Conclusions

(a) The optimization process that has been used in the present work proved to be a favorable approach for determining optimum radii of curvatures of various lenses in each optical system.

(b) The results concerning the optical parameters of the various systems that have been obtained by ZEMAX are found to be in good agreement with those determined by Visual Basic computer program.

(c) Designs show acceptable values of dimensions and specifications indicate that these optical systems are feasible.

(d) Design1 and Design2 have a big distortion in the image wavefront as shown in figures (3.2a) and (3.13a) and these designs are not acceptable.

(e) The system that has KRS-5 optical material in its components must be protected.

4.2 Suggestions for future work

Form the results of the present investigation, one may recommend the following projects for future work.

(a) An optimization process for the material for lenses that constitute Four Elements Objective Lens in another arrangement differ that in the present work.

Or an optimization process for the material in order to select another infrared material with regard to paraxial lens parameters and image quality evaluation.

(b) Construction of the various optimized optical systems and testing their performance in experimental infrared systems would offer both verification and justification of the computational work.

1.1 Electromagnetic Spectrum

Many different types of radiations are encountered daily. Seemingly different forms, such as sunlight, heat, radio waves, and x-ray to name only a few, are inherently similar in nature and can be conveniently grouped under a single classification called electromagnetic radiation. It is common practice to describe these radiations by their position in the electromagnetic spectrum – an arrangement of the various radiations by wavelength or frequency. All of the electromagnetic radiations obey similar laws of reflection, refraction, interference, diffraction, and polarization. The electromagnetic radiations differ from one another only in wavelength and frequency [**Hudson 1969**].

The detailed portion of the spectrum that includes the infrared radiation is depicted in table (1.1) and figure (1.1). It is often convenient to subdivide the infrared into four parts. Figure (1.1) shows that the infrared region is bounded on the short wavelength side by the visible light and on the long wavelength by microwaves. Since heated objects radiate energy in the infrared region, it is often referred to as the heat region of the spectrum.

Table (1.1): Subdivision of the infrared [Hudson 1969].

Designation	Abbreviation	Wavelength (μm)
Near infrared	NIR	0.75 to 3
Middle infrared	MIR	3 to 6
Far infrared	FIR	6 to 15
Extreme infrared	XIR	15 to 1000

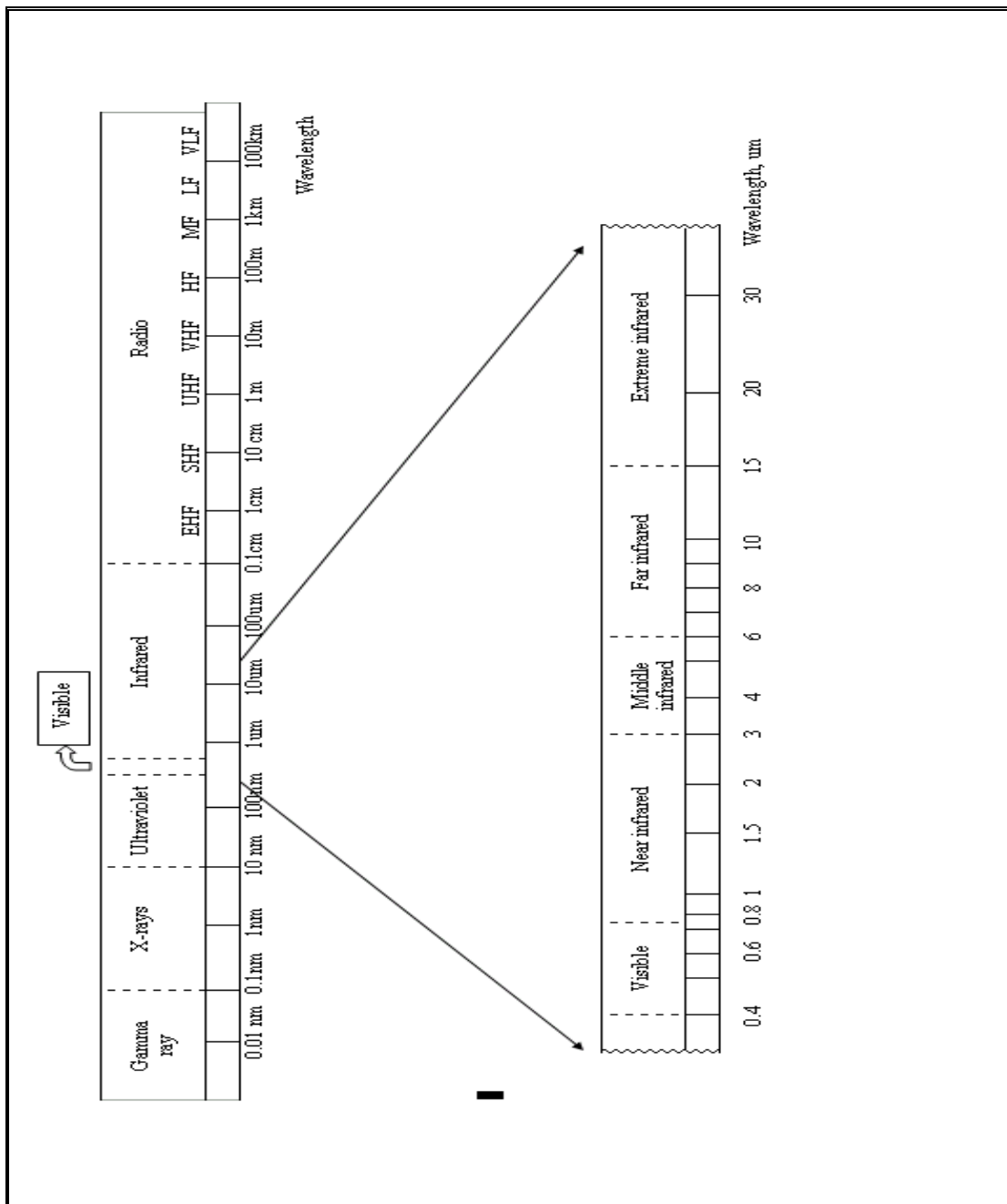


Figure (1.1) The electromagnetic spectrum [Hudson 1969].

1.2 The Lens

The lens is the most basic optical component. It collects light from a source and refracts that light to form a usable image of source. The source may produce light itself or it may be an illuminated object.

The term "lens" is applicable to a number of configurations. The most basic, the simple lens is a single element. The compound lens consist of a group of two or more of simple lenses, and the complex lens is one made up of multiple groups of lens elements [ORIEL 2005]. Figure (1.2) shows the three types of lenses. In the optical system of the present work, the complex lens has been taken into account.

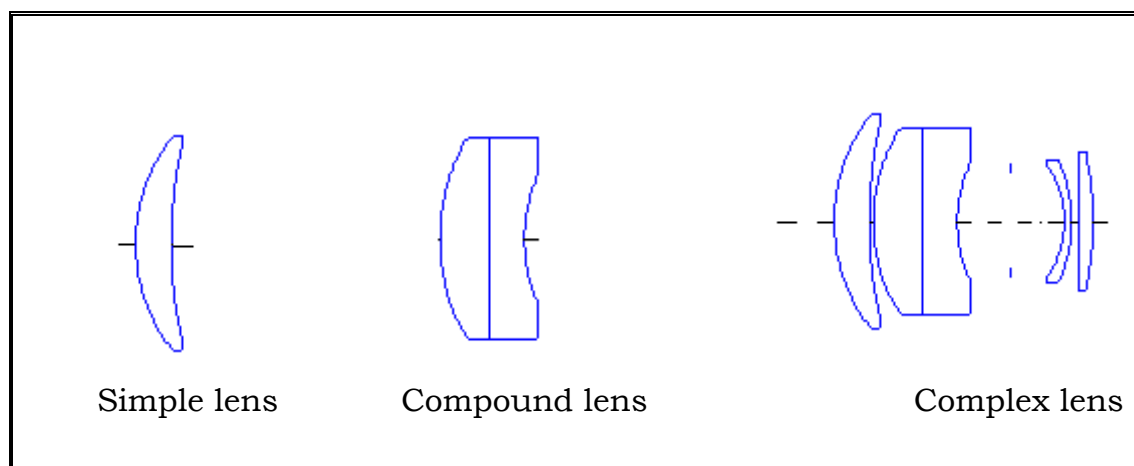


Figure (1.2) Three types of lenses [ORIEL 2005]

The lens is defined by several parameters, the curvature of the surface, the separation of surfaces, and the index of

refraction of medium between the surfaces. If the medium is dispersive, the index of refraction will vary with wavelength, and the dispersive characteristics of the material need to be stated [**Shannon 1997**].

The air gap between adjacent lenses can be regarded as an "air lens" imbedded in glass. In many situations these air lenses, in glass, have glass lens equivalents, in air. The resulting new designs, when certain of the original air lenses are removed, often have distinctly better aberration correction, or other features that are desirable, such as a different system length. This transformation is easiest when the air lens that is to be removed has a nearly concentric meniscus shape. The glass lens equivalent then has about the same shape, and is located outside the two lenses bounding the air gap. The latter disappears and two adjacent lenses combine into a single lens. The air space allows one to use a wide variety of glass types, and still correct for coma. An alternate use of the air gap is to control higher order spherical aberration [**Shafer 1983**].

Infrared lenses differ from lenses designed for the visual region of the spectrum in several important aspects. These differences may be summarized as follows [**Laikin 2001**]:

(a) There are a lot fewer materials to choose from. The available infrared materials have high index of refraction and low dispersion (e.g. germanium, zinc selenide...).

(b) Due to the high cost of these materials and their relatively poor transmission, thickness should be kept to a minimum. Many of these materials are polycrystalline and exhibit some scattering; this is another reason to keep the lens thin.

(c) The long wavelength means a much lower resolution requirement.

(d) The walls of the housing emit radiation and so contribute to the background.

(e) Detectors are often linear arrays, in contrast to film or the eye. These detectors are usually cooled.

(f) One must check that the detector is not being imaged back onto itself.

1.3 Design Requirements of Optical Systems

The optical system design process should be consistent with the required applications. Many applications required some specialized design and a successful optical system design required that the designer always considers the design specifications, which is the most important step in the optical design process. The ordinary design process can be broken down into the following three steps [**Dubner1959**]: **(a)** the choice of the type of design to be executed, that is, the number and types of the elements and their general configuration, **(b)** the determination of the powers, materials, thickness, and spacing of the elements which is usually selected to control the chromatic aberrations of the system, as well as the focal length, working distance, field of view and

aperture, and **(c)** adjustment of the shapes of the various elements or components to correct the basic aberrations to the desired and optically acceptable values.

1.4 Infrared Systems

Due to its importance in the present investigation the optical design of Infrared systems needs to be described. Figure (1.3) illustrates the important elements of an infrared system [**Hudson 1969**].

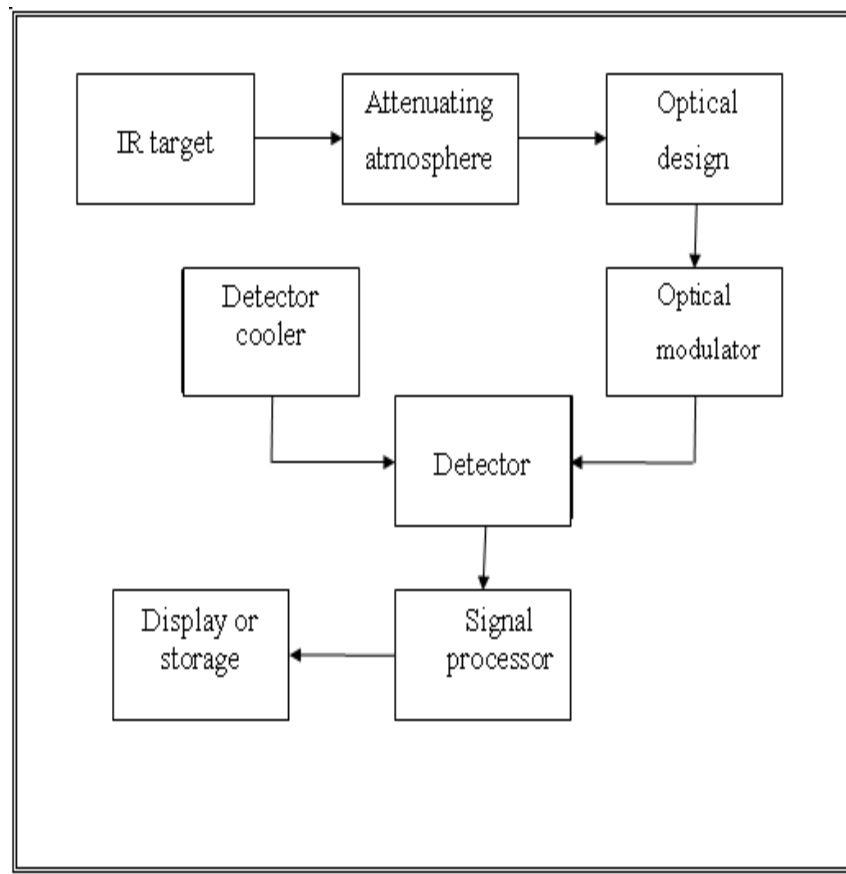


Figure (1.3) Important elements of an infrared system [**Hudson 1969**].

The elements are as follows:

1. Infrared Target.
2. Attenuating Atmosphere where absorption in the atmosphere by H₂O, CO₂ and N₂O causes various windows or regions of transmission. Water vapor is the principle absorber in the 1μm to 4μm region, while carbon dioxide absorbs significantly at 2.7μm and is also the main absorber between 4μm and 5μm. Therefore, the two main infrared windows are 3.2μm to 4.2μm that which used in this investigation and the 8μm to 14μm region [**Laikin 2001**].
3. The optical design of an Infrared system in this investigation represented by **Four Elements Objective Lens** shown in figure (1.4) which is used in the middle infrared waveband MIR (3.2-4.2) μm. The objective of this investigation is realized in a four element infrared objective lens having a forward assemblage and rearward assemblage. The forward assemblage including two lenses; first lens is L₁ and second lens is L₂. The rearward assemblage including two lenses; third lens L₃ and fourth lens L₄. This optical system needs the lenses from L₁ to L₄ being axially aligned [**Fjeldsted 1983**]. The *entrance pupil* is located between the forward and rearward assemblages and the focus position is away from the fourth element. These features provide a solution for a wide variety of purposes, some of which are disclosing electronic problems in circuit boards, night vision systems, detection of hot bearings on railroad car wheels and intended to

provide a best solution for a high resolution thermal imaging and having the smallest size and least weight [Laikin 2001].

4. Cooled or uncooled detection system.
5. Signal processor
6. Display

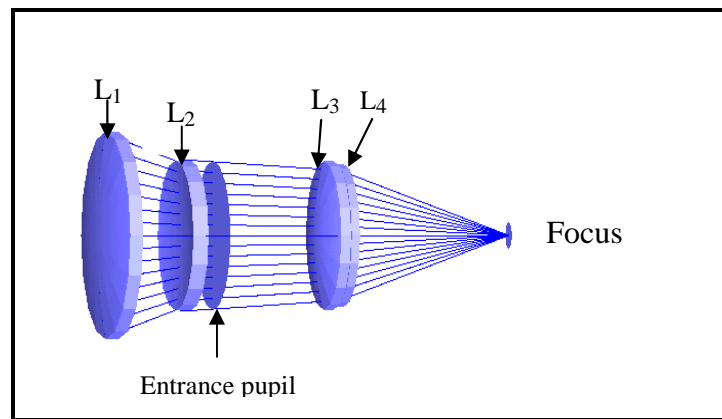


Figure (1.4) Four Element Objective Lens [Laikin 2001]

1.5 Literature Survey

Modern infrared technology was born during the Second World War in the twentieth century. In its early years, infrared technology was financially supported chiefly by military funds and was directed toward military applications. Thus technical details were protected by military security and were not released for general civilian use; that is, the literature of infrared technology was largely classified and was unavailable to the scientific and engineering fraternities. The security barrier was gradually lowered, and in the late 1950's and early 1960's books on

infrared techniques began to appear. Concurrently the technical journals printed more and more infrared articles, and professional societies scheduled papers on infrared physics and technology [**Hudson1969**]. In spite of the available information on infrared technology in the published literature, the fine details concerning theory and experiment are either still classified or not declared clearly. Thus, a survey concerning this subject is considered poor when the advances and applications are taken into account.

The infrared objective lens is an important element in one optical infrared system. In the following, a brief literature survey is presented which covers mostly inventions and studies in foreign countries and postgraduate dissertations accomplished in Iraq on some optical systems.

Four element infrared objectives invented by **Sijgers (1967)** that invention relates to infrared optics and more particularly, to a novel infrared lens system that combines large aperture, moderate depth of field, focal length, high resolution and small field curvature in unprecedented way. **Kirkpatrick (1969)** invented a Far Infrared Lens relates to infrared optics, and more particularly to an objective lens operable in the region of 8 - 15 μ m for focusing a substantial field of view onto a flat image plane. In a more specific aspect, the invention relates to a far infrared objective lens in which none of the surfaces are a spherical.

Rogers (1977) designed two optical systems consisted from four elements of different materials one operated in FIR 8 - 14 μm and the other operated in MIR 3 – 5 μm .

Fjeldsted (1983) invented a Four Element Infrared Objective Lens design provided having lenses of crystalline semiconductor materials such as silicon and germanium. An infrared objective lens system 3.3 – 4.2 μm comprises a primary lens group which made of material the refractive index in which is relatively temperature insensitive such as arsenic triselenide and / or zinc selenide and this a primary lens group air spaced from a secondary lens group, their materials having a refractive index which is relatively temperature insensitive such as arsenic triselenide and temperature sensitive such as germanium, this system invented by **Neil (1985)**. At the same year an infrared objective system lens has been designed by **Boutellier (1985)** which provides an infrared lens system for the wavelength range of 3.5 - 5 μm , that design consists of three lens elements made from silicon, calcium fluoride and silicon respectively, such design intended for use in a thermal imaging device.

The suitability of zinc sulfide versus germanium for the middle negative lens of the Cooke triplet design for the 3 – 5 μm spectral region is studied by **Sharma (1992)**. In **2000 Norrie** invented an objective lens system uses germanium lens elements. Also **Sadiq (2000)** investigated

optical systems using the ray tracing analysis to compute wavefront aberrations. The ZEMAX computer program was used by **Zahed (2000)** to design and analyze the homing head systems for tracking targets that emit IR radiation. In **(2004) Zain Al-Abedeem** studied the atmospheric effects on 3 - 5 μm band thermal imaging. The Requirements of the optical elements for IR laser range finder were investigated computationally by **Albakir (2005)**.

In our project Four Element Objective Lens are designed and operated at MIR region (3.2 – 4.2 μm). Some elements materials have been used to show their suitability for that design.

1.6 Aim of the Work

The present work aims to put forward an optical design of a MIR system for many applications. The essential parameters that are required in an optical system such as ray tracing analysis, paraxial lens formulas, spot size, intensity distribution, and fraction of encircled energy would be investigated and analyzed. The quality of the proposed design would be investigated using various types of optical elements materials in order to improve its performance in Infrared system applications.

1.7 Work Objective

The main steps that have been adopted in order to execute the present research objective are as follows:

- (a)** Suggest optical systems designs for an Infrared system based on the example found in literature [**Laikin 2001**] one by choosing a different optical material comport with the design and its application.
- (b)** Optimize the suggested system design for the selected optical materials with merit function by ZEMAX program.
- (c)** Study the suggested system design analytically by determining the effective parameters and their roles.
- (d)** Determine the parameters with the aid of computer program specifically written for the optical system depending on the physical equations and the significance of these parameters.

2.1 Introduction

The process of optical design is both an art and a science. There is no closed algorithm that creates a lens, nor there is any computer program that will create a useful lens designs without general guidance from an optical designer. The mechanics of computation are available with a computer program, but the inspiration and guidance for useful solution to a customer's problems come from the lens designers. The most successful design includes a blend of techniques and technologies that meet the goals of the customer. This final blending is guided by the judgment of the designer [**Shannon 1997**].

With so many different optical components available, the task of choosing the right elements for any particular optical system can be seemed daunting. However, for many applications, few simple calculations will enable one to select the appropriate optics, or at very least, yield a narrow list of choices.

The process of solving virtually any optical engineering problem can be broken down into main steps. In the first step, paraxial calculations are made to determine critical quantities such as magnification, focal length(s), clear aperture (diameter), and object and image positions. The next part of solving optical problem involve by choosing actual components based on the paraxial values, and then

evaluating their real world performance, particularly the effects of aberrations. Truly rigorous performance analysis for all but simplest optical systems generally requires computer ray tracing, but again, simple generalizations can be used, especially when the lens selection process is limited to a certain range of component shapes. In practice, the performance evaluation stage may reveal conflicts with design constraints, such as component size, cost, and product availability. In this case, system parameters may have to be modified [**Griot 2004**].

2.2 Paraxial Optics

Paraxial optics is used to determine the location and size of image and pupils in the optical system. Sometimes, this is referred to as first-order optics or Gaussian optics. The paraxial quantities provide information about ideal image formation in selected set of coordinates. Paraxial variables are angles and ray coordinates that describe the passage of a paraxial ray through the lens. These angles may be selected in object space to correspond to the sine or tangent of the real ray angles that will pass through the lens.

Paraxial rays are always very close and nearly parallel to the optical axis. In this region, lens surfaces are assumed normal to the axis, and hence all angles of incidence and refraction are small. As a result, the sine of the angles of

incidence and refraction are small and can be approximated by the angles themselves measured in radians.

2.2.1 Paraxial equations

Figure (2.1) shows a ray of light leaving an object point P and striking the first surface of lens at point P₁. It is refracted and proceeds to the second surface at point P₂. The amount of refraction is specified by Snell's law equation (2.1) [Nssbaum 1998]

$$n_1 \sin \theta = n'_1 \sin \theta' \quad (2.1)$$

where n_1 and n'_1 are the refractive indices of different optical media separating by surface, and θ and θ' are the angle of the ray before and after refraction at separating surface. The trigonometric function sine can be expressed as a Taylor series equation (2.2) this has the form

$$\sin \theta = \theta - \frac{\theta^3}{3!} + \frac{\theta^5}{5!} - \dots \quad (2.2)$$

where the angle θ is expressed in radians. For small values of θ , only the first term on the right side of equation (2.2) needs to be used,

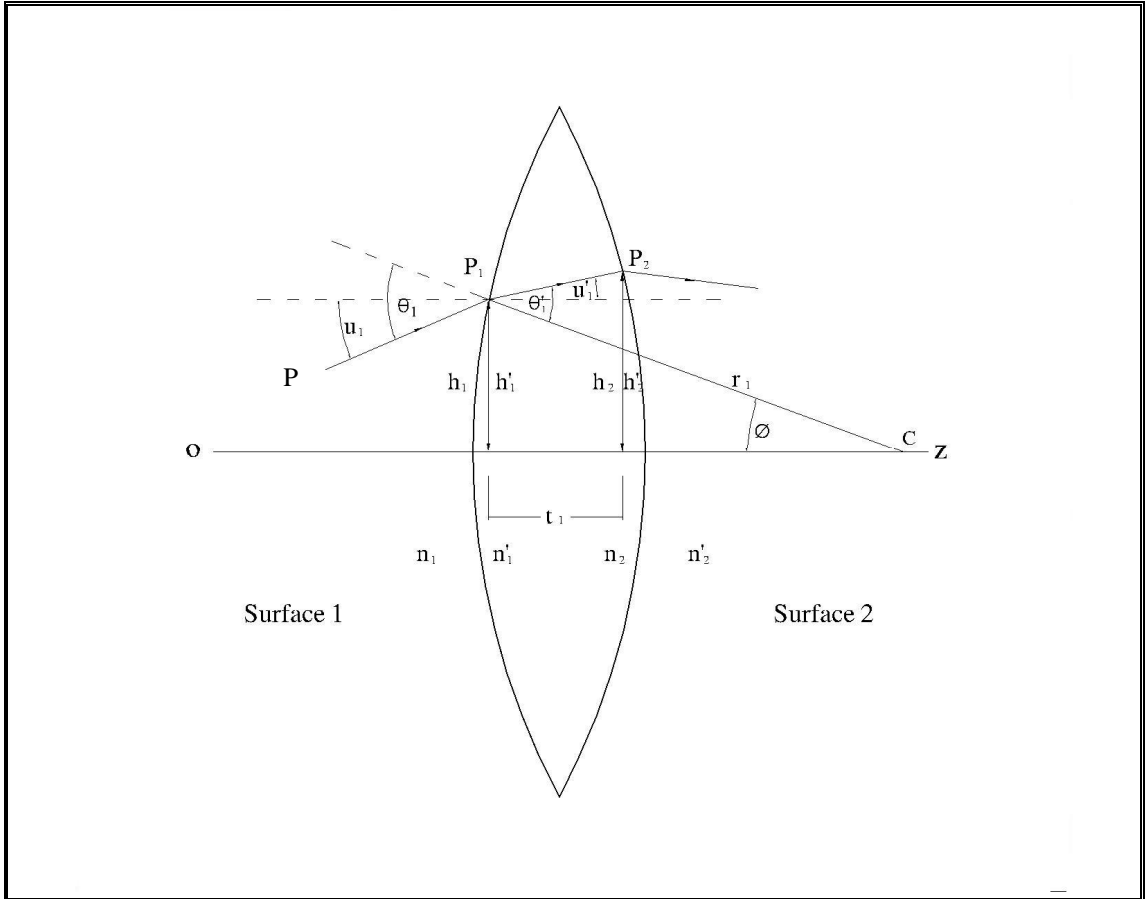


Figure (2.1) Shows a ray of light pass through lens surfaces [Nussbaum 1998]

then the Snell's law simplified to

$$n_1 \theta_1 \cong n'_1 \theta'_1 \quad (2.3)$$

this is called the paraxial form of Snell's law, however, Snell's law angles are not convenient to work with, and eliminate with the identities

$$\theta_1 = u_1 + \phi \quad (2.4)$$

$$\theta'_1 = u'_1 + \phi \quad (2.5)$$

where u_1 is the angle of the incident ray as considered with the parallel to optical axis, u'_1 is the corresponding angle for the refracted ray, and ϕ is the angle that the radius r_1 of the lens surface makes at the center of curvature Cc. this particular angle can be simplified as

$$\sin \phi = \frac{h_1}{r_1} \quad (2.6)$$

from paraxial approximation one can simplify equation (2.6), to obtain

$$\phi = \frac{h_1}{r_1} \quad (2.7)$$

Substituting (2.4), (2.5) and (2.7) in (2.3), the result can be written as

$$n_1' u_1' = \frac{n_1 - n_1'}{r_1} h_1 + n_1 u_1 \quad (2.8)$$

the distance from point P_1 to the axis is labeled as h_1 and K_1 is called the refracting power of the *surface 1* and is defined as

$$K_1 = \frac{n_1' - n_1}{r_1} \quad (2.9)$$

the curvature c_1 of lens *surface 1* is defined as

$$c_1 = \frac{1}{r_1} \quad (2.10)$$

then equation (2.9) may also written as

$$K_1 = c_1 (n_1' - n_1) \quad (2.11)$$

and equation (2.8) written as

$$n_1' u_1' = n_1 u_1 - K_1 h_1 \quad (2.12)$$

as the ray goes from P_1 to P_2 , its distance from the axis becomes

$$h_2 = h_1 + t_1 \tan u_1' \quad (2.13)$$

or, using the paraxial approximation for small angles

$$h_2 = h'_1 + t_1 u' \quad (2.14)$$

2.3 Ray Tracing

An introduction to the use of lenses in solving optical applications can begin with the elements of ray tracing [Newport 2004]. Ray tracing is widely used in optical system design. In the basic form, ray tracing propagates a number of rays through a proposed optical system, using the exact geometrical results of Snell's law and the law of refraction at each interface. In this sense there are no approximations, and the ray trajectories are 'exact', showing the lens user the true system performance. There are three types of rays in spherical systems: paraxial rays, meridional rays, and skew rays. In the present work only the paraxial ray tracing used in optical systems where the rays are traced from surface to surface in a predefined sequence. Tracing rays sequentially means a ray will start at surface 0, then be traced to surface 1, then to surface 2, etc. No ray will be traced from surface 5 to 3 even if the physical location of these surfaces would make this the correct path [ZEMAX 1999].

This process of finding a ray path in terms of the numerical values of the incidence heights and convergence angles at each surface in turn is called *ray tracing* and it is of fundamental importance in optical design. This importance comes from that the results obtained are used in

aberration calculations in addition to yielding the Gaussian properties.

First, the surfaces and spaces have to be numbered consistently. Suppose there are k refracting or reflecting surfaces; they are numbered from the left, using the number as subscript, so that c_j is the curvature of the j^{th} surface. The refractive indices of the media preceding and following c_j are n_j and n_j' respectively. The axial distance from c_j to c_{j+1} is d_j' , taken as positive if c_{j+1} is to the right of c_j , as is usual. The symbol d_{j-1} would denote the distance from c_j to c_{j-1} and it would usually be negative but this is not often required. There is some redundancy of symbols, since $n_j' = n_{j+1}$ and $d_j' = -d_{j+1}$.

Figure (2.2) shows an optical system with the ray segments numbered according to the scheme [**Welford 1974**]. It can be seen from this figure that the ray segment incident at surface j is specified by h_j and u_j' , so that the incidence heights and convergence angles are generalized coordinates of the ray as it passes through the optical system, as in equations (2.11), (2.12), and (2.14).

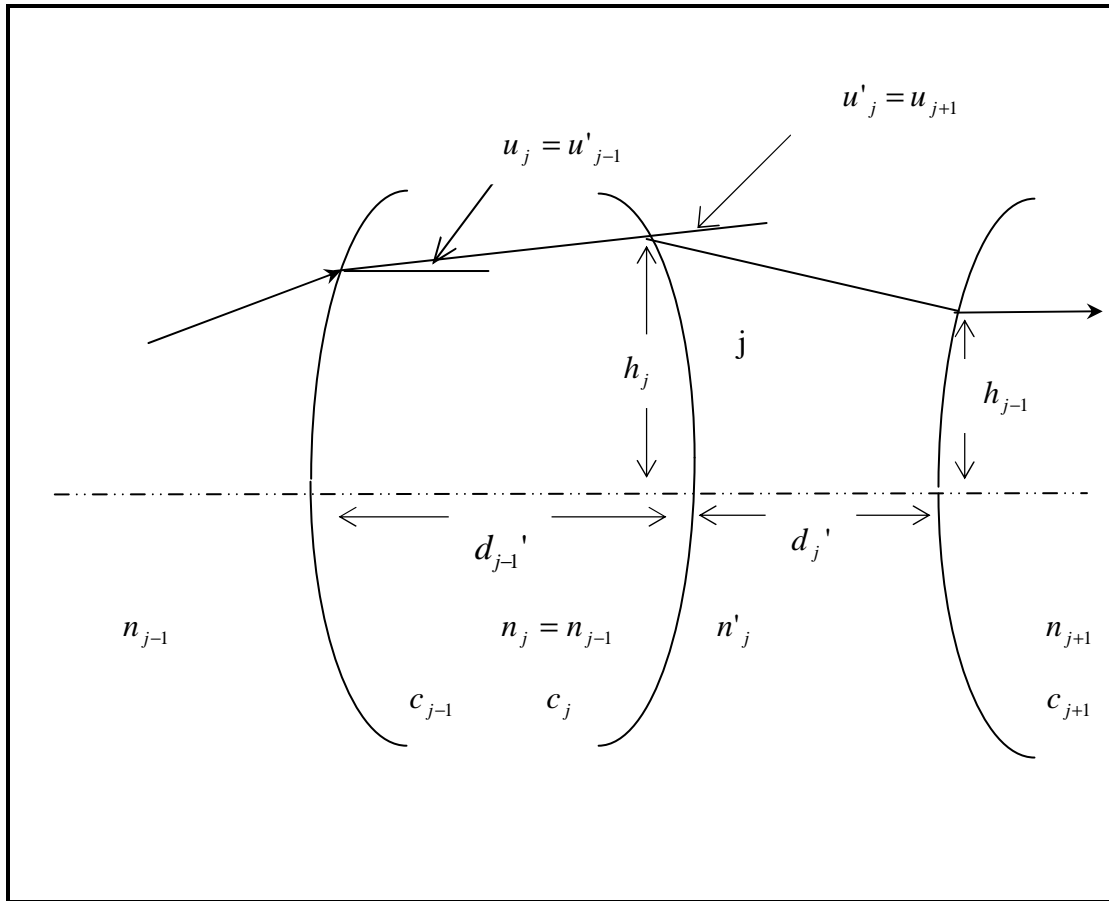


Figure (2.2) A scheme of notation for paraxial ray tracing [Welford 1974].

The surface powers K_j , refractive indices, etc., are given; thus if one starts from u_j and h_j the equations given above in section (2.2.1) can be applied in succession to obtain u_{j+1} and h_{j+1} , and so on through the system. Equation (2.3) is called the *refraction equation* and equation (2.5) is the *transfer equation*. Those two are thus a set of recurrence formulae, to be applied numerically. The effective focal length *efl* and back focal length *bfl* corresponding to the paraxial formula are given by [Welford 1974],

$$efl = \frac{-h_1}{u'_k \cdot n'_k} \quad (2.15)$$

$$bfl = \frac{h_k}{u'_k} \quad (2.16)$$

where h_1 is the ray height on *surface 1*, u'_k is the last ray angle, n'_k is the last element index, and h_k is the last ray height.

The paraxial effective focal length calculated at infinite conjugates over the paraxial entrance pupil diameter is called F-number and it is named also lens speed and symbolized by $(f/\#)$. Note that infinite conjugates are used to define this quantity even if the lens is not used at infinite conjugates. It is a useful indicator of the brightness of the image produced by the source far from the lens. It is defined as [**ZEMAX 1999**]

$$f/\# = \frac{f}{D} \quad (2.17)$$

where D is the diameter of lens aperture, f is the focal length.

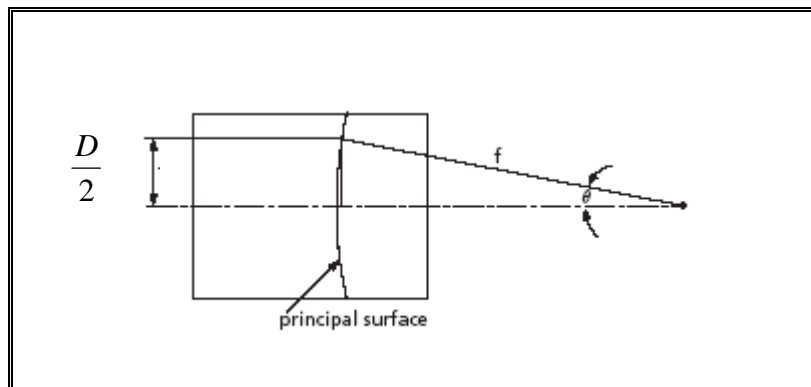


Figure (2.3) F-number and numerical aperture [**Griot 2004**].

The term used commonly in defining the cone angle is numerical aperture. Numerical aperture (NA) is the sine of the angle made by the marginal ray with the optical axis. By referring to figure (2.3) and using simple trigonometry, it can be seen that [**Griot 2004**],

$$NA = \sin \theta = \frac{D}{2f} \quad (2.18)$$

or

$$NA = \frac{1}{2(f/\#)} \quad (2.19)$$

Note that the *aperture* means the diameter of the largest entering beam of light which can travel through the system.

When looking through a binocular, the widest dimension of circular viewing area that one can see is described as the field of view. The concept of angular field of view (*FOV*) is important when the usable image size is limited. *FOV* is the angle subtended by the source producing the maximum usable image size; it is given by [**Griot 2004**],

$$FOV = 2 \tan^{-1} \left(\frac{\text{image} \cdot \text{height}}{efl} \right) \quad (2.20)$$

2.4 Seidel Aberration Sum

It's important to mention the Snell's refraction invariant before introducing Seidel aberration formulae for spherical aberration. From figure (2.1) and equations from (2.3), to (2.7) one get

$$n_1(u_1 + hc_1) = n(u_1' + hc_1) \quad (2.21)$$

either side of equation (2.21) is denoted by A and this quantity is called Snell's refraction invariant. So, this invariant is essentially a paraxial quantity and it is, only invariant before and after refraction at a given surface.

According to [**welford 1974**]

$$A = nu_1 + nhc_1 \quad (2.22)$$

and

$$\bar{A} = n\bar{u}_1 + n\bar{h}c_1 \quad (2.23)$$

in terms of the data of ray tracing of the paraxial ray (u and h) as shown in figure (2.2), the primary aberration sum for spherical aberration given by [**Weleford1974**]

$$S_I = - \sum_{all-surfaces} A^2 h \Delta \left(\frac{u}{n} \right) \quad (2.24)$$

where the symbol Δ refers to change of the quantities enclosed by the parentheses.

Now recalling the definition of the power of thin lens given by equation (2.11), and need to specify the symmetrical shape or bending variable of the lens and the conjugates or magnification variable which are defined as follows [**Weleford1974**]

Shape or bending variable

$$B = \frac{n_o(n-1)(c_1 + c_2)}{K} = \frac{c_1 + c_2}{c_1 - c_2} \quad (2.25)$$

Conjugate or magnification variable

$$C = \frac{n_o(u_1 + u'_2)}{hK} = \frac{u_1 + u'_2}{u_1 - u'_2} \quad (2.26)$$

these are dimensionless, also normalized (division by K). The relations between the variables and curvatures and convergence angles given by [**Weleford1974**]

$$\left. \begin{aligned} c_1 &= \frac{K}{2n_o(n-1)}(B+1) \\ c_2 &= \frac{K}{2n_o(n-1)}(B-1) \\ u_1 &= \frac{hK}{2n_o}(C+1) \\ u'_2 &= \frac{hK}{2n_o}(C-1) \end{aligned} \right\} \quad (2.27)$$

to calculate the Seidel sum for a thin lens , by tracking a symbolic ray tracing through the lens, as done in

section (2.3) substituting in equation (2.24) and then replacing u , c , A by their equivalents in the thin lens variables as obtain from equations (2.27).

The powers of the individual surface are $n_o(n-1)c_1$ and $-n_o(n-1)c_2$; the ray trace gives the convergence angle inside the lens $n(u_1 - (n-1)c_1h)/n_o$ and for the final convergence angle $u'_2 = u_1 - hK/n_o$.

Thus obtained:

$$\begin{aligned}
 -S_I = n_o(hc_1 + u_1)^2 h \left[\frac{u_1 - (n-1)hc_1}{n^2} - u_1 \right] \\
 + n_o(hc_2 + u'_2)^2 h \left[u'_2 - \frac{u_1 - (n-1)hc_1}{n^2} \right]. \quad (2.28)
 \end{aligned}$$

Next substitute from equations (2.27) gives

$$S_I = \frac{h^4 K^3}{4n_o^2} \left[\left(\frac{n}{n-1} \right)^2 + \frac{n+2}{n(n-1)^2} \left(B + \frac{2(n^2-1)}{n+2} C \right)^2 - \frac{n}{n+2} C^2 \right] \quad (2.29)$$

These expressions enable the designer to make modification to his design since they involve some degrees of freedom (the refractive indices, and curvature) to minimize aberrations [**Welford 1974**].

2.5 Optical Lens Materials

Glass manufacturers provide hundreds of different glass types with differing optical transmissibility and mechanical strengths. There are, however, two instances in which one might need to know more about optical materials: one might need to determine the performance of a catalog component in a particular application, or one might need specific information to select a material for a custom component [Griot 2004]. The most important material properties to consider in regard to an optical element are as follows:

- (a) index of refraction
- (b) thermal characteristics
- (c) mechanical characteristics
- (d) chemical characteristics, and
- (e) cost.

Furthermore, the optical properties that are most important are as follows

- (a) transmission
- (b) refractive index and dispersion, and
- (c) homogeneity.

Crystalline materials are often used in optics application because of their unique optical and physical properties. Their high translucence in the UV and IR spectral regions, and wide variety of the dispersion properties, permit

a considerably wider choice of application as compared with optical glasses [**ISP Optics 2005**].

The valuable optical properties of certain natural crystals have been recognized for years, but the usefulness of these materials has been severely limited by the scarcity of pieces of the size and quality required for optical applications. However, many crystals are available in synthetic form. They are grown under carefully controlled conditions to size and clarity otherwise unavailable [**Smith 1966**].

Particular attention has been paid to the strong influence of the various materials on the performance of the infrared optical systems under consideration. Some of the physical and chemical properties of the infrared optical materials that are most important in the present work are given in Appendix I and as follows:

(a) Germanium and silicon

Germanium (Ge) and silicon (Si) are widely used for refracting elements in infrared devices. Silicon is very much like glass in its physical characteristics, and can be processed with ordinary glass working techniques. Both are metallic in appearance, being completely opaque in the visible. Their extremely high index of refraction is of importance to the lens designer since the weak curvatures which result tend to produce designs of a quality which cannot be duplicated in comparable glass systems [**Smith 1966**].

(b) Zinc Selenide

Zinc Selenide (ZnSe) is used for optical windows, lenses, mirrors and prisms particularly for infrared applications. The transmission range is 0.5 - 22 μm . Zinc Selenide is produced by synthesis from zinc vapour and H_2Se gas, forming as sheets on graphite susceptors. It is microcrystalline in structure, the grain size being controlled to produce maximum strength. Single crystal ZnSe is available, because having lower absorption and thus more effective infrared optics. [**Crystal Techno 2005**]

(c) Thallium Bromiodide (TlBr-TlI) (KRS-5)

Thallium bromiodide KRS-5 (TlBr-TlI) is used for attenuated total reflection prisms, infrared windows and lenses where transmissions in the 0.6 - 40 μm range is desired. It has a tendency to cold-flow and changes its shape with time. KRS-5 is only slightly soluble in water but can be dissolved in alcohol, nitric acid, and aqua regia. This material is considered toxic and should be handled with care. [**Crystal techno 2005**]

(d) AMTIR-1

AMTIR-1 ($\text{Ge}_{33}\text{As}_{12}\text{Se}_{55}$ Glass) is an amorphous infrared transmission material. It is most economical for an infrared lens. It is manufactured from AMTIR-1 synthetic material. It was originally produced for night vision systems, but is has other applications including optical elements and optical

sensors for remote temperature sensing. The transmission range of AMTIR-1 750nm to 14 μ m, and its refractive index is 2.6055 at 1.0 μ m, and 2.4977 at 10.0 μ m [**ICL 2003**].

2.6 Diffraction Effects

In all light beams, some energy is spread outside the region predicted by rectilinear propagation. This effect, known as diffraction, which is a fundamental and inescapable physical phenomenon. Diffraction can be understood by considering the wave nature of light. Huygens's principle states that each point on a propagating wavefront is an emitter of secondary wavelets as shown in figure (2.8). The combined focus of these expanding wavelets forms the propagating wave. Interference between the secondary wavelets gives rise to a fringe pattern that rapidly decreases in intensity with increasing angle from the initial direction of propagation. Huygens's principle describes diffraction [**Griot 2004**].

Diffraction effects are traditionally classified into either Fresnel or Fraunhofer types. Fresnel diffraction is primarily concerned with what happens to light in the immediate neighborhood of a diffracting object or aperture. It is thus only of concern when the illumination source is close to this aperture or object.

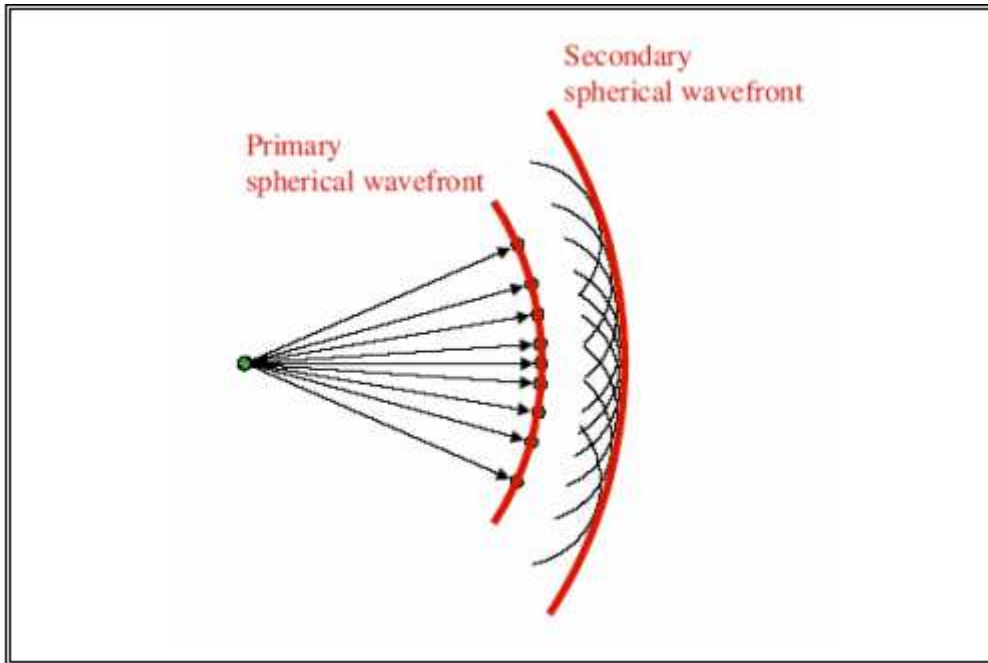


Figure (2.4) Huygens's principle diagram [Griot 2004]

Consequently, Fresnel diffraction is rarely important in most optical setups [Griot 2004]. Fraunhofer diffraction, however, is often very important. This is the light spreading effect of an aperture when the aperture (or object) is illuminated with an infinite source (plane-wave illumination) and the light is sensed at an infinite distance (far-field) from this aperture. From these overly simple definitions, one might assume that Fraunhofer diffraction is important only in optical systems with infinite conjugate, where as Fresnel diffraction equations should be considered at finite conjugate ratios. A lens or lens system of finite positive focal length with plane-wave input maps the far field diffraction pattern of its aperture appears onto the focal plane; therefore, it is Fraunhofer diffraction that determines the limiting performance of optical systems [Griot 2004].

2.6.1 Fraunhofer diffraction at circular aperture

Fraunhofer diffraction at a circular aperture dictates the fundamental limits of performance for circular lenses. It is important to remember that the spot size, caused by diffraction, of a circular lens is

$$d = 2.44\lambda f / \# \quad (2.30)$$

where d is the diameter of the focused spot produced from plane wave illumination and λ is the wavelength of light being focused. It can be seen that the f-number of the lens, not its absolute diameter that determines this limiting spot size.

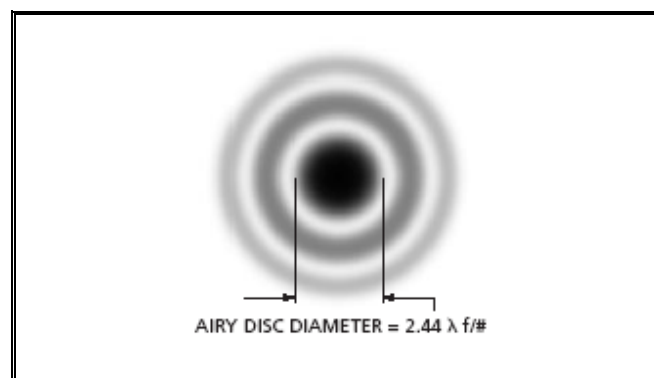


Figure (2.5) Center of typical diffraction pattern for a circular aperture

The diffraction pattern resulting from a uniformly illuminated circular aperture actually consists of a central bright region, known as the Airy disc shown in figure (2.9), which is surrounded by a number of much fainter rings. Each ring is separated by a circle of zero intensity. The irradiance distribution in this pattern can be described by **[Born and Wolf 1980]**

$$I(r) = I_0 \left(\frac{2J_1(kra)}{(kra)} \right)^2 \quad (2.31)$$

at the center $r=0$, and

I_0 = Peak of intensity distribution in image.

J_1 = First-order Bessel function.

a = Radius of circular aperture.

For comparison purposes, the intensity of diffraction pattern of circular aperture uniformly illuminated can also be written in terms of the zero-order Bessel function J_0 **[Wynat 1992]**.

$$I(r) = I_{\max} \left| \int_0^1 J_0[(kar)\rho] \rho d\rho \right|^2 \quad (2.32)$$

where ρ = radial coordinate for the exit pupil. It is usually normalized with respect to spot radius.

The intensity of diffraction pattern of circular aperture having a rotationally symmetric pupil function $(\delta(\rho))$, which is illuminated with a uniform beam, is

$$I(r) = I_{\max} \cdot \left| \int_0^1 \delta(\rho) \cdot J_0[(kar) \cdot \rho] \rho \cdot d\rho \right|^2 \quad (2.33)$$

For spherical aberration, the rotationally symmetric pupil function is

$$\delta(\rho) = \exp(i \frac{2\pi}{\lambda} W_{040} \rho^4) \quad (2.34)$$

where W_{040} = wavefront aberration coefficient for spherical aberration, its equal $\frac{1}{8} S_1$,

If defocus is included, then [**Wyant 1992**],

$$\delta(\rho) = \exp(i \frac{2\pi}{\lambda} (W_{040} \rho^4 + W_{020} \rho^2)) \quad (2.35)$$

$W_{020} = \pm \lambda / 4$ wavefront aberration coefficient for focus, its first-order properties of the wavefront and is not Seidel aberration.

2.6.2 Spot size

Theoretical equation (2.39) gives the half spot size of the spot formed by Fraunhofer diffraction of circular aperture of single lens under aberration-free conditions.

If one deals with an optical system, some modifications should be imposed on equation (2.39) to correct the computed spot size formed by optical system. The modification includes the addition of the aberration term. Hence, the size of the spot formed by an optical system can be calculated from the following equation [**Scott 1959**]

$$SpotSize = 2.44\lambda(f/\#) + \frac{Tf}{(f/\#)^3} \quad (2.36)$$

where T is a constant given by the following expression [**Scott 1959**],

$$T = \frac{n+2}{n(n-1)^2} B^2 - \frac{4(n+1)}{n(n-1)} B + \frac{3n+2}{n} + \frac{n^2}{(n-1)^2} \quad (2.37)$$

and $B = \frac{r_2 + r_1}{r_2 - r_1}$

B is the shape or bending variable and n being the refractive index of the last surface.

2.7 Fraction of Encircled Energy (FEE)

The fraction of encircled energy (FEE) within a specific diameter region on the image surface is a measure of the energy concentration. Computation of this quality is carried out by choosing a center of coordinates and then carrying out the integration over the intensity distribution. The choice of the center of coordinates for intensity distribution that are symmetric, the center can be chosen to maximize the energy within each energy area [Shannon1997]. So, a fraction of the total incident energy is contained within the central core of the diffraction pattern. Denoting by $FEE(r_0)$ the fraction of the total energy contained within a circular radius r_0 in the image surface centered on the geometrical image, one may have [Born & Wolf 1980]

$$FEE(r_0) = \frac{1}{E_{tot}} \int_0^{r_0} \int_0^{2\pi} I(r) r dr d\phi \quad (2.38)$$

where $I(r)$ = intensity distribution of diffraction pattern of a circular aperture of radius r . For aberration-free condition the fraction of incident energy contained within the central core of the diffraction pattern within a circle of radius r_0 in the image plane, centered on the geometrical image, given by

$$FEE(r_0) = 1 - J_0^2[kar] - J_1^2[kar] \quad (2.39)$$

2.8 Merit Function

The merit function is a numerical representation of how closely system meets a specified set of goals; the ideal situation is a merit function that considers the boundary conditions for the lens as well as the image defects. These boundary conditions include such items as maintaining the effective focal length or (magnification), $f/\#$, center and edge spacing, over all length, pupil location, element diameters, location on the glass map, paraxial angle controls, and the paraxial height controls [**Shannon 1997**].

The merit function is proportional to the squares of the difference between the actual and target boundary condition values as shown in equation () [**Shannon 1997**]

$$MF^2 = \sum_{i=1}^{i=n} W_i Dd_i^2 \quad (2.40)$$

where MF = Merit function.

W = Weight of defect items to permit control of image.

Dd = The defect item (difference between the actual and target boundary condition).

n = Number of defect item.

2.9 Optimization

Optimization consists of adjusting the parameters of a lens to meet as closely as possible the requirements placed on the design. The process of optimization requires the selection of a starting point and a set of variables. Reducing the magnitude of the merit function should indicate that the design is closer to the desired solution [**Shannon 1997**].

Any parameter describing the lens could be used as a variable. Usually only a subset of the available is used in order to maintain some control over the properties and configuration of the lens. The most important variables are the curvatures of the surfaces. Usually the designer will elect to use the "radius of curvature," which is easier to visualize, as it is the physical quantity that will be measured in building the lens [**Shannon 1997**].

The next type of variable is the separation between optical surfaces. This can be the thickness of element, or air space between the elements (air lens). In some cases, thickness can be infinitesimal, indicating that the two surfaces of lenses are contact or cemented. In general, if left unbounded lenses will usually expand to fill all of the available space during a design. Therefore, the thickness variables should always be bounded. The defects will usually change slowly with changes in axial thickness, so

thickness may or may not be useful variable [**Shannon 1997**].

The optical properties of the materials used in a lens can obviously be variable. Usually, the optical glasses used will be established at the beginning for cost, delivery, or environmental reasons. The materials must be replaced by the closest available material and optimization run completed with specified material in order to have a physically viable lens [**Shannon 1997**].

CONTENTS

Certification	ii
Examination Committee Certification	iii
Acknowledgment	iv
Synopsis	v
List of Symbols and Abbreviations	viii

Chapter one (*INFRARED LENS DESIGN*)

1.1 Electromagnetic Spectrum	1
1.2 The Lens	3
1.3 Design Requirements of Optical Systems	5
1.4 Infrared System	6
1.5 Literature Survey	8
1.6 Aim of the Work	11
1.7 Work Objective	12

Chapter two (*OPTICAL CONSIDERATIONS*)

2.1 Introduction	13
2.2 Paraxial Optics	14
2.2.1 Paraxial equations	15
2.3 Ray Tracing	19
2.4 Seidel Aberration Sum	24
2.5 Optical Lens Material	27
2.6 Diffraction Effects	30
2.6.1 Franhofer diffraction at circular aperture	32

2.6.2 Spot size	35
2.7 Fraction of Encircled Energy	36
2.8 Merit Function	37
2.9 Optimization	38
Chapter Three (RESULTS AND DISCUSSION)	
3.1 Design Consideration	40
3.2 Design Optimization	42
3.3 Designs Results	42
3.3.1 Ray tracing analysis	45
3.3.2 Paraxial lens formula	47
3.3.3 Image quality evaluation	49
Chapter Four (CONCLUSIONS AND SUGGESTIONS FOR FUTURE WORK)	
4.1 Conclusions	75
4.2 Suggestions for Future Work	76
REFERENCES	77
APPENDICES	82

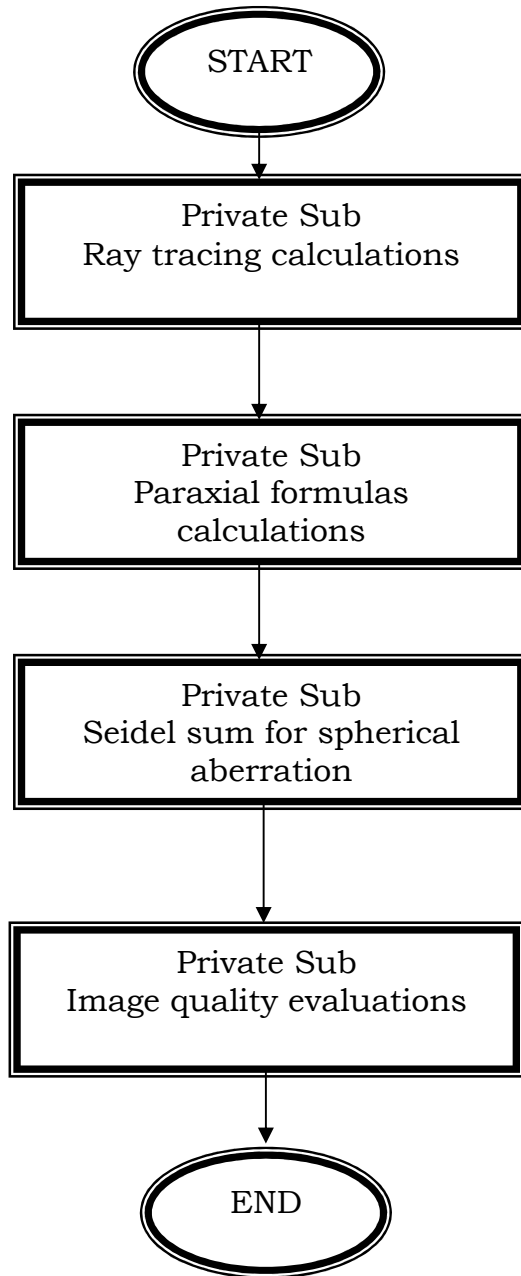
LIST OF SYMBOLS AND ABBREVIATIONS

<u>Symbols</u>		<u>Units</u>
a	Radius of circular aperture	(cm)
A	Refraction invariant	
AMTIR-1	Amorphous material transmission infrared	
B	Shape or bending constant	
bfl	Back focal length	(cm)
c	Curvature	(cm ⁻¹)
Cc	Center of curvature	
C	Conjugate or magnification constant	
d	Axial separation between the optical element	(cm)
Dd	Design defect	
D	Diameter of aperture	(cm)
E_{tot}	Total energy incident upon the aperture	(joule)
efl	Effective focal length	(cm)
f	Focal length	
FOV	Field of view	(mm)
FEE	Fraction of encircled energy	
f/#	F-number	

G ($\mathbf{x}_o, \mathbf{y}_o$)	Pupil function	
Ge	Germanium	
h	Paraxial incidence height	(cm)
I	Intensity	(watt/cm ²)
J₀, J₁	Zero and first order Bessel function, respectively	
k	Wave number	(μm^{-1})
K	Lens power	(Diopter)
KRS-5	Thallium Bromoiodide	
LCA	Longitudinal chromatic aberration	
MF	Merit function	
n	Refractive index	
P₁, P₂	Points on lens surfaces	
P_o, P	Points on aperture and image plane	
r_i	Radius of curvatures	(cm)
r	Radius of circle centered at image plane	(cm)
S_I	Primary aberration sum for spherical aberration	
T	Spot size aberration constant	
t	Center thickness of optical element	(cm)

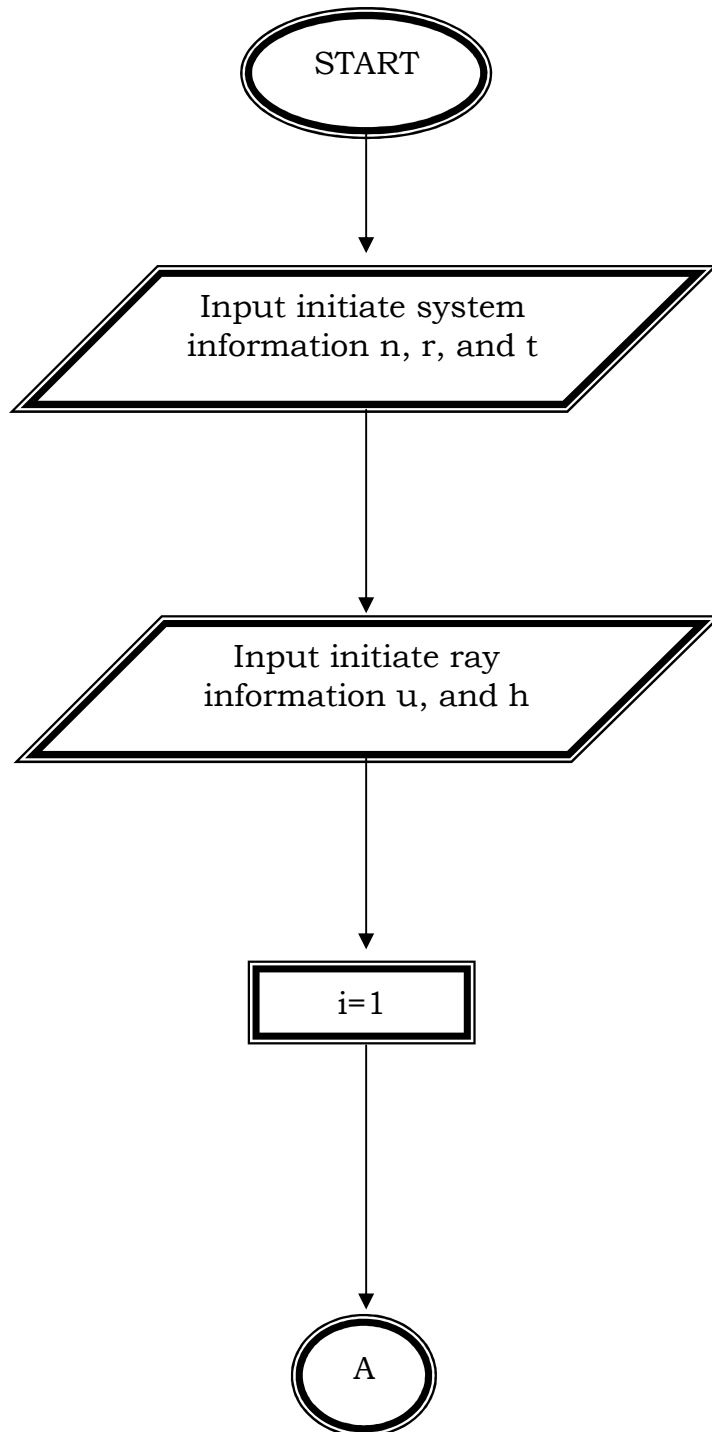
TCA	Transverse chromatic aberration	
u	Paraxial convergence angle	(rad)
V	Abbe number	
W₀	Pupil function constant	
W	Calculation weight	
W₀₄₀	Wavefront aberration constant	
W₀₂₀	Wavefront aberration constant	
ZnSe	Zinc selenide	
λ	Wave length	(μm)
θ	Angle of incident	(degree)
δ(ρ)	Rotational symmetrical pupil function	

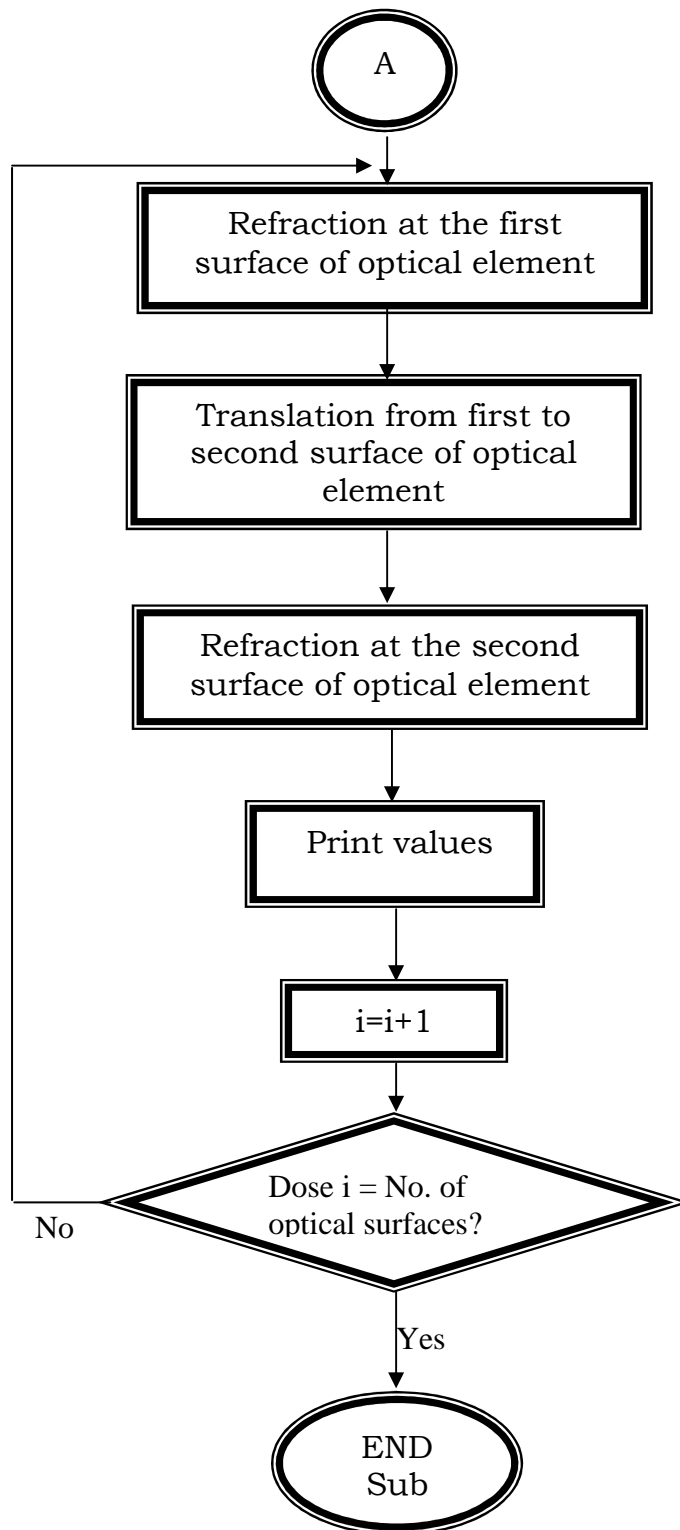
Main Program Flow Chart



Sub Program Flow Chart

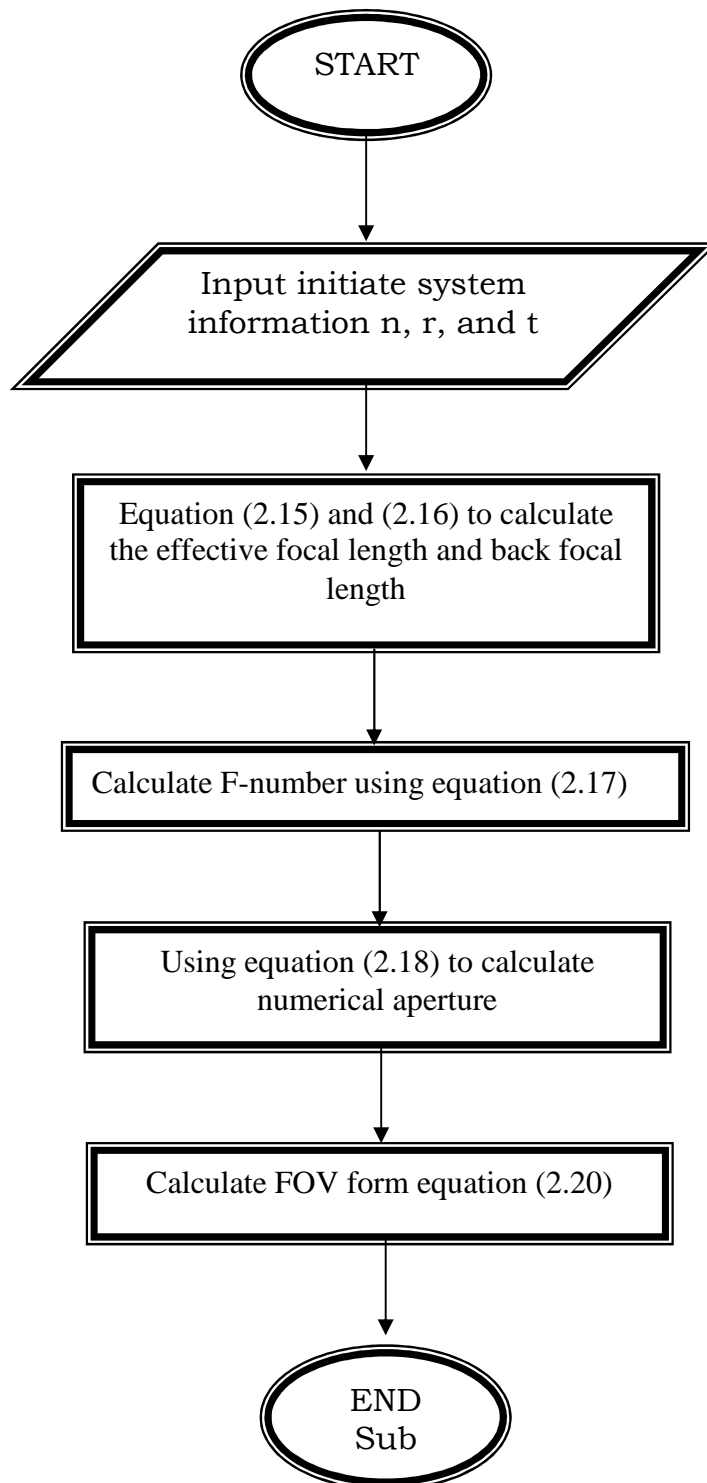
Ray tracing





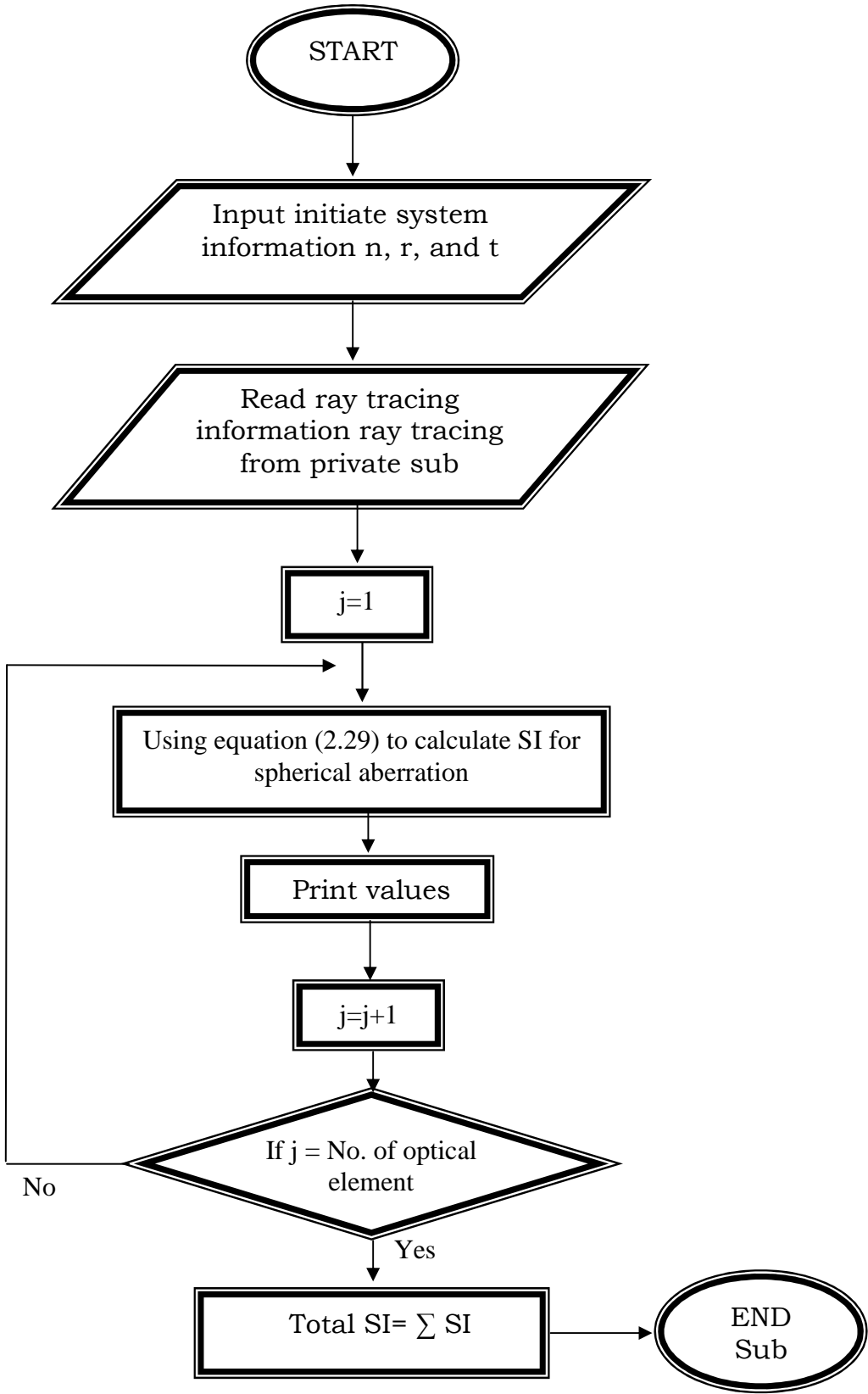
Sub Program Flow Chart

Paraxial lens formulas



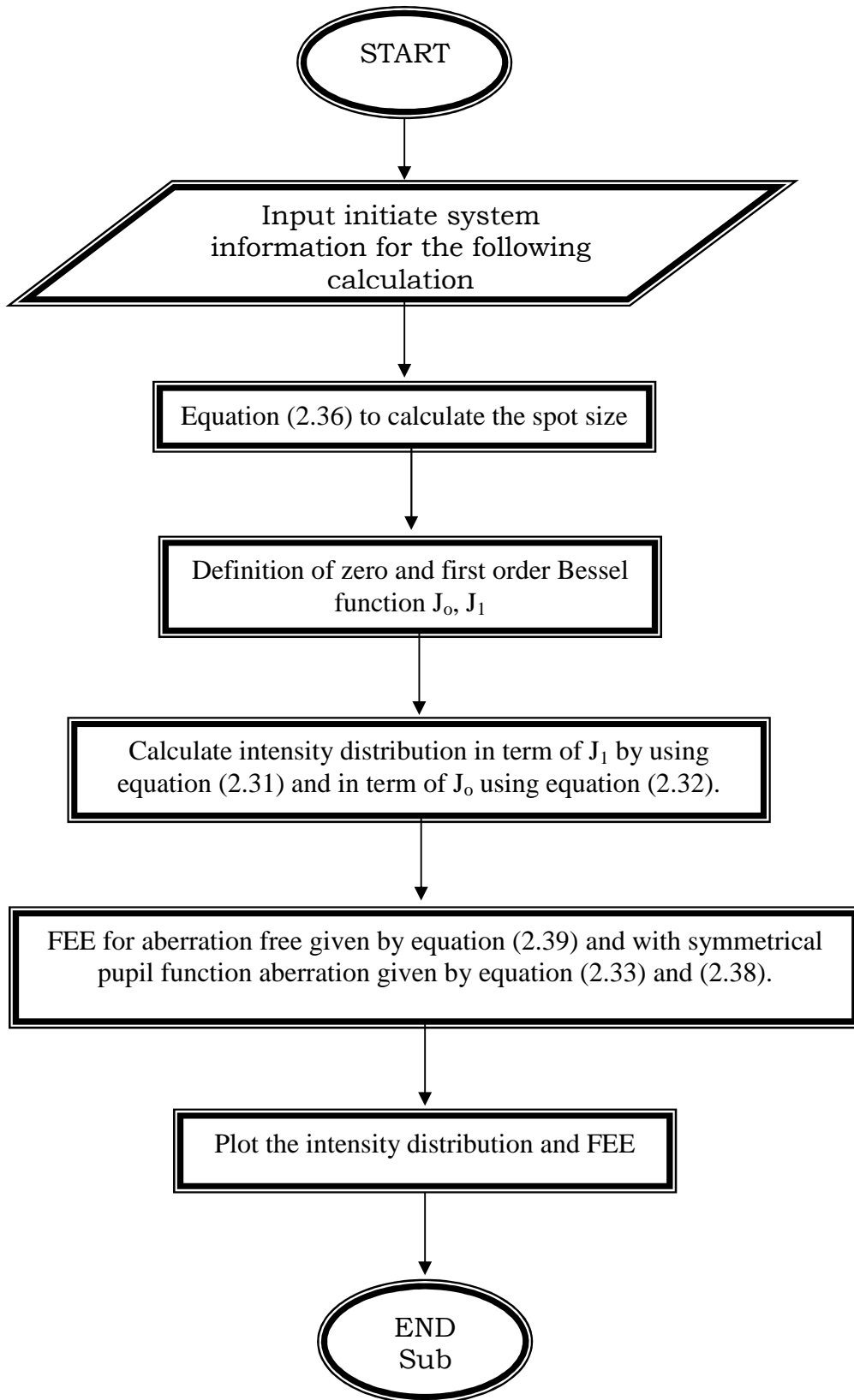
Sub Program Flow Chart

Seidel sum for spherical aberration



Sub Program Flow Chart

Image quality evaluations

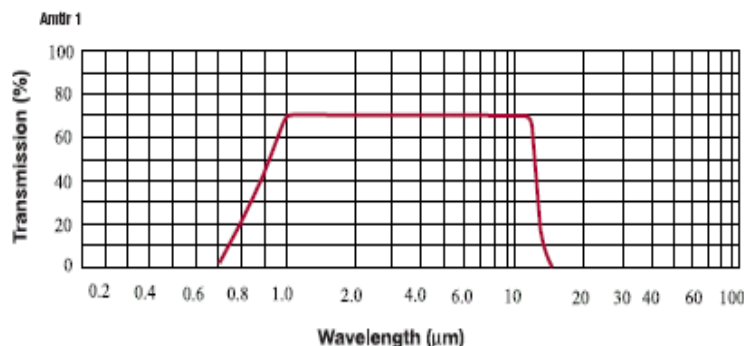


AMTIR-1 (Amorphous Material Transmitting Infrared Radiation)

AMTIR-1 is a “glass like” amorphous material with a high homogeneity, that is able to transmit in the infrared. AMTIR-1 is used for infrared windows, lenses, and prisms, when transmission in the range of .75-14µm is desired. AMTIR-1 is not water soluble. The low thermal change in refractive index ($72 \times 10^{-6}/^{\circ}\text{C}$) is an advantage in lens design to prevent defocussing. The upper use temperature is 300°C.

AMTIR-1's composition of Ge₃₃As₁₂Se₅₅ makes it somewhat similar to Germanium in its mechanical and optical properties. It is nearly as dense as Germanium but has a lower index of refraction, making it a good option for color correction with Germanium in an optical system. AMTIR-1 performs especially well in the 8-12µm spectral region where its absorption and dispersion are the lowest. AMTIR-1 optical grade material is generally more expensive than Germanium.

Property	Specification
<i>Transmission Range</i>	.75µm to 14µm
<i>Density</i>	4.4 g/cm ³
<i>Thermal Expansion Coefficient</i>	12x10-6 / °C
<i>Surface Finish</i>	Typical specifications for surface quality in the infrared are 40-20 or 60-40 scratch dig in the 1 to 7 µm spectral region and 60-40, 80-50 or 120-80 scratch-dig for the 7-14µm area, depending upon system performance requirements. Diamond Turned surface finishes of 120 Angstroms rms or better are typical.
<i>Surface Figure</i>	In the infrared, typical required surface figure ranges from 1/2wave to 2 waves @0.6328 µm depending on the system performance requirements.
<i>AR Coating Options</i>	Mostly BBAR coated for use in the 3-5µm or 8-12µm spectral regions. Many other specialized coating bands are possible between 1 and 14µm.
<i>Typical Applications</i>	Thermal imaging, FLIR, YAG laser systems.
<i>Products Manufactured</i>	Lenses, Aspheric Lenses, Binary (Diffractive) Lenses, Windows, Wedges, Prisms.



Wavelength µm	Index of Refraction (n)
1.00	2.606
2.00	2.531
3.00	2.519
4.00	2.514
7.00	2.506
10.00	2.498
14.00	2.483

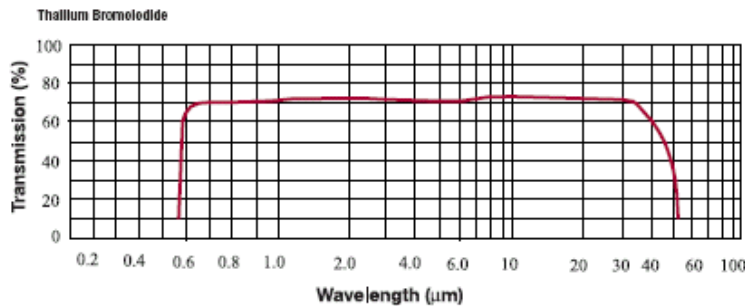
Thallium Bromiodide (KRS-5)

Thallium Bromiodide is widely used for optics when transmission to about 40 μ m is desired. KRS-5 is relatively insoluble in water and may be used in cells in contact with aqueous solutions.

KRS-5 is superior to the simple Bromide and Iodide Salts in that it is much harder. The top operating temperature is 200°C. The material does not cleave but will flow under pressure. The softness of the material limits the optical figure and surface quality that can be achieved in fabrication.

Property	Specification
Transmission Range	0.6 μ m to 40 μ m
Density	7.371 gm/cc
Thermal Expansion	58x10 ⁻⁶ /°C

Surface Finish	Generally a Low Scatter Polish for the Infrared (80-50 Scratch Dig).
AR Coating Options	Moisture Protection (Specify Wavelength of Use).
Typical Applications	Attenuated total reflection prisms, IR windows and lenses.
Products Manufactured	Windows, Lenses, Wedges, Prism, Aspheric Lenses, Beam Splitters.



Wavelength μ m	Index of Refraction (n)
2.0	2.395
4.0	2.382
6.0	2.378
8.0	2.375
10.0	2.371
12.0	2.366
14.0	2.364
16.0	2.355
18.0	2.348
20.0	2.341
22.0	2.332
24.0	2.323
26.0	2.312
28.0	2.301
30.0	2.289
32.0	2.275

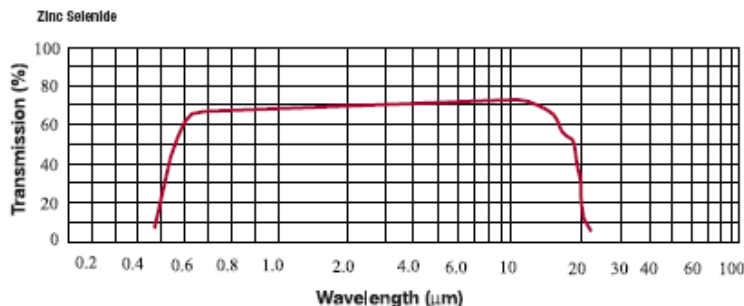
Zinc Selenide (ZnSe)

Zinc Selenide is used for infrared windows, lenses, and prisms where transmission in the range 0.63 μm to 18 μm is desired. Zinc Selenide has a very low absorption coefficient and is used extensively for high power infrared laser optics. It is non-hygroscopic.

Zinc Selenide is a relatively soft material and scratches rather easily. The low absorption of the material avoids the thermal runaway problems of Germanium. Zinc Selenide requires an anti-reflection coating due to its high refractive index if high transmission is required. ZnSe has a fairly low dispersion across its useful transmission range.

Zinc Selenide, a chemically vapor deposited material, is the material of choice for optics used in high power CO₂ laser systems due to its low absorption at 10.6 μm . However it is also a popular choice in systems operating at various bands within its wide transmission range. ZnSe has a high resistance to thermal shock making it the prime material for high power CO₂ laser systems. ZnSe however is only 2/3 the hardness of ZnS multi-spectral grade but the harder anti-reflectance coatings do serve to protect ZnSe. Zinc Selenide's cost is about the same as ZnS multi-spectral grade and is generally more expensive than Germanium.

Property	Specification
<i>Transmission Range</i>	0.6 μm to 16 μm
<i>Density</i>	5.27g/cm ³
<i>Thermal Expansion Coefficient</i>	7.1x10 ⁻⁶ /°K @ 273°K, 7.8x10 ⁻⁶ /°K @ 373°K, 8.3x10 ⁻⁶ /°K @ 473°K
<i>Surface Finish</i>	Typical specifications for surface quality in the infrared are 40-20 or 60-40 scratch dig in the 0.8 to 7 μm spectral region and 60-40, 80-50 or 120-80 scratch-dig for the 7 to 16 μm area, depending upon system performance requirements. Diamond Turned surface finishes of 150 Angstroms rms or better are typical.
<i>Surface Figure</i>	In the infrared, typical required surface figures range from 1/2 wave to 2 waves @0.6328 μm depending on the system performance requirements.
<i>AR Coating Options</i>	Typical available coatings for ZnSe include BBAR for 0.8 to 2.5 μm , 3 to 5 μm , 1 to 5 μm , 8 to 12 μm , and the 3 to 12 μm spectral regions and single wavelength coating AR at 10.6 μm . Many other specialized wavelength bands are possible within the 0.6 to 16 μm range.
<i>Typical Applications</i>	CO ₂ laser systems, Thermal imaging, FLIR, Astronomical, Medical
<i>Products Manufactured</i>	Lenses, Aspheric Lenses, Binary (diffractive) Lenses, Windows, Optical Beamsplitters and Optical Filters, Prism.



Wavelength μm	Index of Refraction (n)
1.0	2.4890
3.0	2.4380
4.0	2.4330
5.0	2.4300
7.0	2.4220
9.0	2.4120
10.6	2.4028
11.0	2.4000
13.0	2.3850
15.0	2.3670
17.0	2.3440

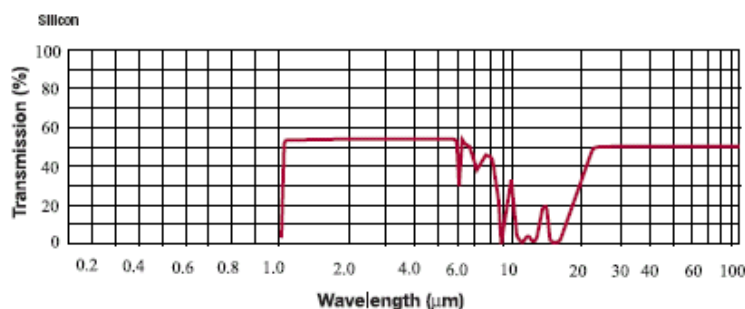
Silicon (Si)

A semiconductor material that is commonly used in infrared optical systems operating in the 3 to 5 μm spectral band. The refractive index is near 3.4 throughout the range. Silicon is also useful as a transmitter in the 20 μm to 300 μm range.

Silicon is used as a mirror substrate for lasers because of its thermal conductivity, light weight, and hardness. It is also used for windows and lenses in the 1.2 μm to 6.7 μm range. Due to the strong absorption at 9 μm , Silicon is not suitable for use with CO₂ lasers as a transmitting optic but is widely used for CO₂ mirrors.

Silicon has one of the lowest densities of the common infrared materials making it ideal for systems with weight constraints. The density of Silicon is only half that of Germanium, Gallium Arsenide and Zinc Selenide. Silicon is harder than Germanium and not as brittle. Silicon is the lowest material cost option of all the infrared materials.

Property	Specification
<i>Transmission Range</i>	1.2 to 7.0 μm and from 25 μm out to beyond 300 μm
<i>Density</i>	2.329 g/cm ³
<i>Thermal Expansion Coefficient</i>	2.55x10 ⁻⁶ /°C@25°C
<i>Surface Finish</i>	Typical specifications for surface quality in the infrared are a 40-20 scratch dig in the 1.2 to 3 μm spectral region and 60-40 scratch-dig for the 3-7 μm area. Diamond Turned surface finishes of 120Angstroms rms or better are typical.
<i>Surface Figure</i>	In the infrared, typical required surface figure ranges from 1/2 wave to 2 waves @0.6328 μm and are usually specified depending on the system performance requirements.
<i>AR Coating Options</i>	The most common anti-reflectance coating for Silicon is BBAR for 3 to 5 μm . Many other specialized wavelength bands are possible within the 1.2 to 7.0 μm range.
<i>Typical Applications</i>	Thermal imaging, FLIR.
<i>Products Manufactured</i>	Lenses, Aspheric Lenses, Binary(Diffractive) Lenses, Windows, Optical Beamsplitters, Optical Filters, Wedges.

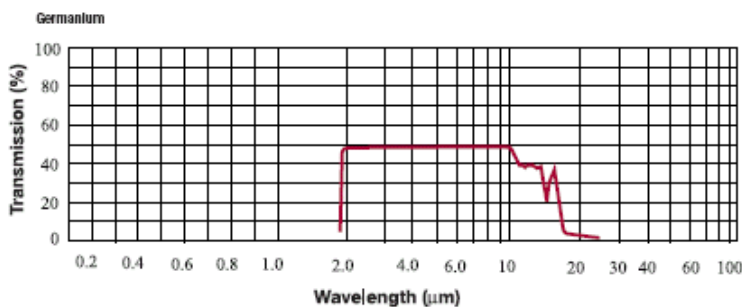


Wavelength μm	Index of Refraction (n)
1.5	3.484
2.0	3.456
3.0	3.436
4.0	3.429
5.0	3.426
6.0	3.424
7.0	3.423

Germanium (Ge)

Germanium has the highest index of refraction of any commonly used infrared transmitting materials. It is a very popular material for systems operating in the 3-5 or 8-12 μm spectral regions. Germanium blocks UV and visible light and in the infrared up to about 2 μm . Its high index is desirable for the design of lenses that might not otherwise be possible. Germanium has nearly the highest density of the infrared transmitting materials and this should be taken into consideration when designing for weight restricted systems. Germanium is subject to thermal runaway, meaning that the hotter it gets, the more the absorption increases. Pronounced transmission degradation starts at about 100 $^{\circ}\text{C}$ and begins rapidly degrading between 200 $^{\circ}\text{C}$ and 300 $^{\circ}\text{C}$, resulting in possible catastrophic failure of the optic.

Property	Specification
Transmission Range	2 to 14 μm
Density	5.33g/cm ³
Thermal Expansion Coefficient	2.3x10 ⁻⁶ / $^{\circ}\text{K}$ @ 100 $^{\circ}\text{K}$, 5.0x10 ⁻⁶ / $^{\circ}\text{K}$ @ 200 $^{\circ}\text{K}$, 6.0x10 ⁻⁶ / $^{\circ}\text{K}$ @ 300 $^{\circ}\text{K}$
Surface Finish	Typical specifications for surface quality in the infrared are 40-20 or 60-40 scratch dig in the 2 to 7 μm spectral region and 60-40, 80-50 or 120-80 scratch- dig for the 7-14 μm area, depending upon system performance requirements. Diamond turned surface finishes of 120 Angstroms rms or better are typical.
Surface Figure	Surface figure: In the infrared, typical surface figure ranges from 1/2 wave to 2 waves @0.6328 μm depending on the system performance requirements.
AR Coating Options	Typical available coatings for Germanium include BBAR for 3 to 5 μm , 8 to 12 μm , and the 3 to 12 μm spectral regions. Many application specialized bands are possible between the 2 and 14 μm .
Typical Applications	Thermal imaging, FLIR.
Products Manufactured	Lenses, Aspheric Lenses, Binary (Diffractive) Lenses, Windows, Optical Beamsplitters, Optical Filters, Wedges.



Wavelength μm	Index of Refraction (n)
2.5	4.046
3.0	4.044
4.0	4.025
8.0	4.007
10.0	4.005
12.0	4.004
14.0	4.003

References

Al-Bakir, Z. T. (2005)

Design Analysis for the Optical Elements of Solid State Laser Range Finder
M.Sc. Thesis, College of Engineering, Al-Nahrain University, Baghdad.

Born, M. and Wolf, E. (1980)

Principles of Optics, Electromagnetic Theory of Propagation, Interference, and Diffraction of Light 6th ed.
(Pergamon Press: Rochester).

Boutellier, R. (1985)

Infrared Objective System Lens
(U.S. Patent #4537464).

Crystal Techno (2005)

Crystal Technology
Via internet: <http://www.chystaltechno.com>.

Ditton, R. (1998)

Modern Geometrical Optics.
(John Wiley: New York).

Dubner, H. (1959)

Optical Design for Infrared Missile-Seekers
(Proceeding of The IRE, June 30 1959)

Fjeldsted, T. P. (1983)

Four Element Infrared Objective Lens
(U.S. Patent #4380363).

Hecht, E. (1998)

Optics 3rd ed.
(Addison Wesley: New York).

Hept, G. B. (2000)

The Chaotic Development of Infrared System for Tactical Aviation
Via Internet: Thesis, Air University
(Air College: Alabama).

Hudson, R. D. (1969)

Infrared System Engineering
(John Wiley: New York), p 14, 20.

ICL (2003)

International Crystal Laboratories
Via Internet: <http://www.icl.com>.

ISP Optics (2005)

General Characteristics of the Material
Via Internet: <http://www.ispoptics.com>.

Jenkins, F. A. and White, H. E. (1976)

Fundamentals of Optics 4th ed.
(McGraw Hill: New York).

Kirkpatrick, T. H. (1969)

Far Infrared Lens
(U.S. Patent #**3439969**).

Laikin, M. (2001)

Lens Design
(Marcel Dekker: New York).

Melles Griot (2000)

Fundamental Optics

Via Internet: <http://www.mellesgriot.com>.

Neil, I. A. (1985)

Infrared Objective Lens System

(U.S. Patent #4505535).

New Port (2004)

Technical Reference, Focusing and Collimating

Via Internet: <http://www.newport.com>.

Norrie, D. G. (2000)

Infrared Objective Lens of Germanium

(U.K. Patent #GB2339303).

Nussbaum, A. (1998)

Optical System Design

(Prentice Hall: USA).

ORIEL INSTRUMENTS

Lens Technical Discussion

Via Internet: <http://www.oriel.com>.

Rogers, P. J. (1977)

Infrared Lenses

(U.S. Patent #4030805).

Sadiq, A. A. (2000)

Computations on Wavefront Aberration Function

M.Sc. Thesis, College of Science, Al-Nahrain University

(Formerly Saddam University), Baghdad.

Scott, R. M. (1959)

Optics for Infrared Systems

(Proceeding of The IRE, June 30 1959)

Shafer, D. (1983)

Optical Design with Air Lenses

(SPIE, **399**), 186-193.

Shannon, R. R. (1997)

The Art and Sciences of Optical Design

(Cambridge University Press: United Kingdom).

Sharma, K. D. (1992)

Some Infrared Materials for The Cooke Triplet Design for the
3-5 μ m Spectral Region: A comparison

(APPLIED OPTICS, Vol. **31**, No. **1**, 1992)

Sijgers, H. J. (1967)

Four Element Infrared Objective

(U.S. Patent #**3321264**).

Smith, F. G. and Thomson, J. H. (1988)

Optics 2nd ed.

(John Wiley: Chichester).

Smith, W. J. (1966)

Modern Optical Engineering (The Design of Optical System)

(McGraw Hill: New York)

Welford, W. T. (1974)

Aberration of the Symmetrical Optical Systems

(Academic Press: London).

Wetherell, W. B. (1980)

Applied Optics and Optical Engineering, Vol. VIII, Chapter Six, The Calculation of Image Quality
(Academic Press: Massachusetts).

Williams, C. S. and Becklund, O. A. (1986)

Optics: A Short Course for Engineering and Scientists
(Robert E. Krieger Publishing Company: Florida)

Wyant, J. C. and Creath, K. (1992)

Applied Optics and Optical Engineering, Vol. XI, Chapter One,
Basic Wavefront Aberration Theory for Optical Metrology
(Academic Press: Arizona).

Zahed, N. K. (2002)

Design and Analysis of an IR Homing Head for Optical Tracking
M.Sc. Thesis, College of Engineering, Al-Nahrain University
(Formerly Saddam University), Baghdad.

Zain Al-Abideen, F. S. (2004)

Atmospheric Effects on 3~5 μm Band Thermal Imaging
Ph.D. Thesis, College of Science, Al-Mustanseriya University Baghdad.

ZEMAX (1999)

ZEMAX Optical Design Program, User Guide, Version 8.0
(March 1999)
(Focus Software: USA).

Acknowledgement

I would like to express my sincere thanks and deep gratitude to **Prof. Dr. Sabah M. Juma** and **Dr. Ahmad K. Ahmad** for supervising the present work and for their support and encouragement throughout the research.

I would like to thank **Mr. Mohamed Saheb** for his valuable assistance during the work.

I am grateful to the Dean of College of Science and the staff of the Department of Physics at Al-Nahrain University for their valuable support and cooperation.

Last but not least, I would like to record my deep affection and thanks to **my parents** for their moral support and patience throughout this work.

Safa'a

Certification

We certify that this thesis entitled “**An Investigation on the Images in Optical Systems of Various Materials**” was prepared by **Mr. Safa’a Abdul Sattar A. Alkaysi**, under our supervision at the College of Science of Al-Nahrain University in partial fulfillment of the requirements for the degree of **Master of Science** in Physics.

Signature:

Name: **Prof. Dr. Sabah M. Juma**

(Supervisor)

Date:

Signature:

Name: **Dr. A. K. Ahamed**

(Supervisor)

Date:

Signature

Name: **Dr. A. K. Ahamed**

(Head of Department)

Date:

Examination Committee Certification

We certify that we have read the thesis entitled “**Design and Analysis of The Four Elements Objective Lens for The 3.2-4.2 μ m Spectral Region**” and as an examination committee, examined the student **Mr. Safa'a Abdul Sattar Auda Al-Kaysi** on its contents, and that in our opinion it is adequate for the partial fulfillment of the requirements of the degree of **Master of Science in Physics**.

Signature:

Name: **Dr. Ayad A. Al-Ani**

Title: **Assistant Professor**

(Chair man)

Date:

Signature:

Name: **Dr. Adawiya J. Haider**

Title: **Assistant Professor**

(Member)

Date:

Signature

Name: **Dr. Fatin A. Al-Moudarris**

Title: **Lecturer**

(Member)

Date:

Signature:

Name: **Dr. A. K. Ahmad**

Title: **Assistant Professor**

(Supervisor and Member)

Date:

Signature:

Name: **Dr. Laith A. Al-Ani**

Title: **Assistant Professor**

(Dean of the College of Science)

Date:

المستخلص

أجري بحث حاسوبي لتصميم منظومه بصريه بأربع عدسات شبيئيه بأستخدام برنامج ZEMAX وكذلك دراسة ملائمة بعض المواد (Si, Ge, AMTIR-1, KRS-5, ZnSe) التي تعمل ضمن منطقة الاشعه تحت الحمراء (3.2-4.2 μm) لعناصر المنظومه البصريه المصممه.

أجريت عملية تحقيق الامثليه لأيجاد بعض الخصائص البصريه والموصفات التصحيحيه الاكثر تفضيلاً من حيث نمط الحيود وحجم البقعه الصوريه الناتجه و كذلك حجم وشكل المنظومه. أن النتائج الحاسوبيه التي تم الحصول عليها بواسطة برنامج ZEMAX أظهرت امكانية استخدام المواد المذكوره ضمن حدود صفاتها البصريه المتمثله بالابعاد البؤريه والزيوغ الكروي وتوزيع الشده والطاقه نسبةً للمنظومه والصور المتكونه عند منطقة التحسس.

تم إجراء مقارنه للنتائج مع التي حسبت بواسطة برنامج Visual Basic وظهر توافقاً عالياً بينهما. أن مواصفات الأنظمه البصريه التي قدمت في البحث الحالي قابل للتنفيذ عملياً.

**Republic of IRAQ
Ministry of Higher Education
and Scientific Research
AL-Nahrain University
College of Science**



DESIGN AND ANALYSIS OF THE FOUR ELEMENTS OBJECTIVE LENS FOR THE 3.2-4.2 μ m SPECTRAL REGION

A Thesis

Submitted to the College of Science of
AL-Nahrain University in Partial Fulfillment of
the Requirements for Degree of Master of Science
in Physics

by

**Safa'a Abdul Sattar A. Alkaysi
(B.Sc. in Physics 2003)**

**Jumada 1
June**

**1427 A.H.
2006 A.D.**



جمهورية العراق
وزارة التعليم العالي والبحث العلمي
جامعة النهرين
كلية العلوم

تصميم وتحليل العدسة الشبئية رباعية العناصر للمدى الطيفي ($4,2-3,2 \mu\text{m}$)

رسالة

مقدمه الى كلية العلوم في جامعة النهرين وهي جزء من متطلبات نيل
درجة ماجستير علوم في الفيزياء

من قبل

صفاء عبد الستار عوده القيسي

(بكلوريوس علوم في الفيزياء ٢٠٠٣)

١٤٢٧ هـ
٢٠٠٦ م

جمادى الأول
حزيران

$$FEE(r_0) = \frac{D}{\lambda^2} \int_0^{r_0} \int_0^{2\pi} \left[\frac{2J_1(kar)}{kar} \right]^2 r dr d\phi \quad (2.47)$$

let

$$\begin{aligned} x = kar, \quad dx = kadr \\ = 2 \int_0^{kar_0} \frac{J_1^2(x)}{x} dx \end{aligned} \quad (2.48)$$

which is a well known recurrence relation

$$\frac{d}{dx} (x^{n+1} J_{n+1}[x]) = x^{n+1} J_n[x] \quad (2.49)$$

or

$$\frac{d}{dx} (x^{-n} J_n[x]) = -x^{-n} J_{n+1}[x] \quad (2.50)$$

Note that

$$J_{-n}[x] = (-1)^n J_n[x] \quad (2.51)$$

from equation (2.48)

$$(n+1)x^n J_{n+1}[x] + x^{n+1} \frac{d}{dx} J_{n+1}[x] = x^{n+1} J_n[x]$$

let $n=0$

$$J_1[x] + x \frac{d}{dx} J_1 = x J_0[x]$$

$$\frac{J_1^2[x]}{x} = J_0[x] J_1[x] - J_1[x] \frac{d}{dx} J_1[x]$$

but from equation (2.49)

$$\frac{d}{dx} J_0[x] = -J_1[x]$$

therefore

$$\frac{J_1^2[x]}{x} = -\frac{1}{2} \frac{d}{dx} (J_0^2[x] + J_1^2[x])$$

and remembering that $J_0[0]=1$ and $J_1[0]=0$, the expression (2.46) now becomes;

Fraunhofer diffraction at circular aperture dictates the fundamental limits performance for circular lenses. The investigation of that type of diffraction must be by using polar instead of rectangular coordinates figure (2.11).

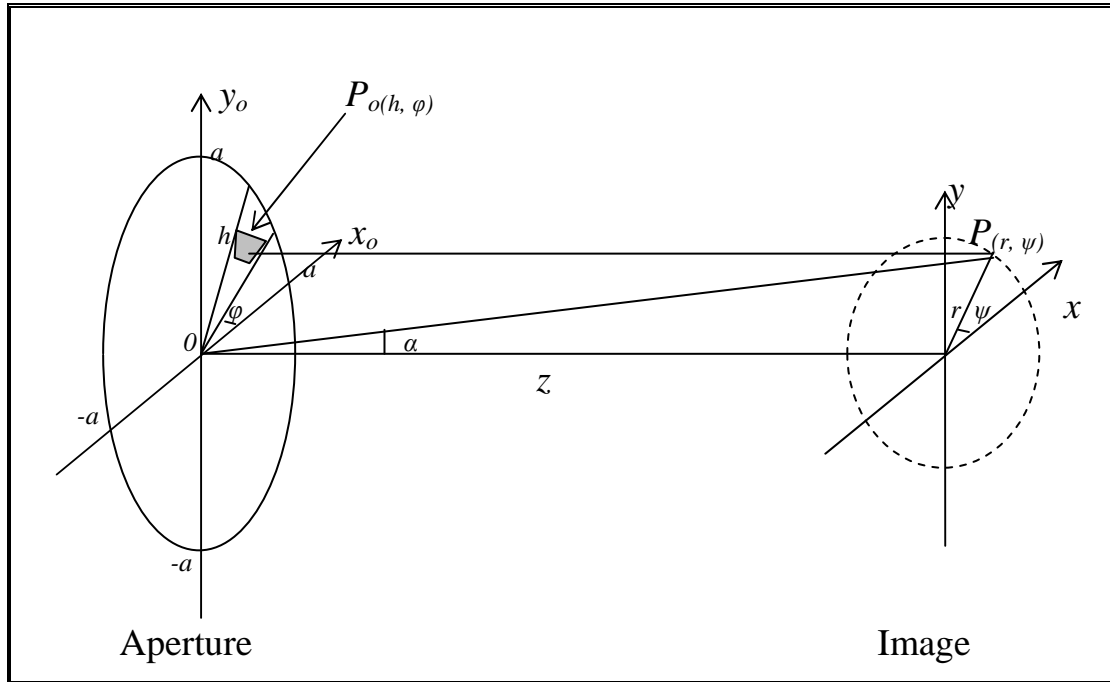


Figure (2.11) Fraunhofer diffraction at circular aperture

Let (h, φ) be the polar coordinates of a typical point on the aperture P_o

$$x_o = h \cdot \cos \varphi$$

$$y_o = h \cdot \sin \varphi$$

and let (r, ψ) be the coordinates of point P in the diffraction pattern, referred to the geometrical image of the source.

$$x = r \cdot \cos \psi$$

$$y = r \cdot \sin \psi$$

the basic integral for Fraunhofer diffraction integral takes the form [**Born and Wolf 1980**]

$$U_P = \iint_s G_{(x_o, y_o)} e^{-ik(x_o + my_o)} dx_o dy_o \quad (2.30)$$

where pupil function $G_{(x,y)}$ given by

$$G_{(x,y)} = \text{constant } (W) \text{ at points in opening}$$

$$G_{(x,y)} = 0 \quad \text{at point outside opening}$$

If a is the radius of the circular aperture, then

$$U_P = \frac{1}{\lambda} \sqrt{\frac{E}{D}} \int_0^a \int_0^{2\pi} e^{-ik\alpha h \cos(\varphi - \psi)} h dh d\varphi \quad (2.31)$$

$$W = \frac{1}{\lambda} \sqrt{\frac{E}{D}}$$

Where E = energy incident upon the aperture.

D = area of the opening.

The φ integral above can be written in term of Bessel function.

$$\int_0^{2\pi} e^{ikrh \cos(\varphi - \psi)} d\varphi = 2\pi J_0(krh) \quad (2.32)$$

where J_0 is the zero-order Bessel function

and

$$\int_0^a J_0(krh) h dh = \frac{J_1(kra)}{(kra)} \cdot a^2 \quad (2.33)$$

where J_1 is first-order Bessel function.

So that equation (2.31) becomes

$$U_p = WD \left(\frac{2J_1(kra)}{(kra)} \right) \quad (2.34)$$

hence the irradiance given by

$$I_p = |U_p|^2 \quad (2.35)$$

$$I(r) = I_o \left(\frac{2J_1(kra)}{(kra)} \right)^2 \quad (2.36)$$

at the center $r=0$

$$I_{\max}(0) = \frac{ED}{\lambda^2} = W^2 D^2 \quad (2.37)$$

so that

$$I(r) = I_{\max} \left(\frac{2J_1(kar)}{(kar)} \right)^2 \quad (2.38)$$

this intensity distribution resulting from a uniformly illuminated circular is generally referred as the Airy pattern. It is actually consists of a central bright region at $r=0$, known as Airy disc shown in figure (2.12), which is surrounded by a number of much fainter rings. Each ring is separated by a circle of zero intensity known as a dark ring.

For first dark ring, $I = 0$ at [**Born and Wolf 1980**].

$$r = 1.22 \frac{\lambda}{2a} \quad (2.39)$$

And the Airy disc diameter $= 2.44 \lambda f / \#$ this value for smallest spot size that can be achieved by optical system with a circular aperture of given f -number.

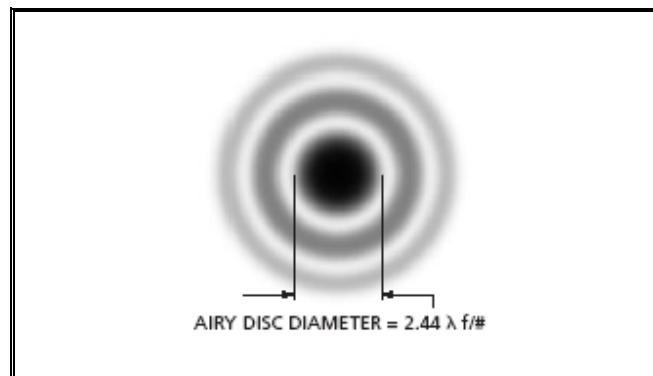


Figure (2.12) Center of typical diffraction pattern for a circular aperture

For comparison purposes, the intensity of diffraction pattern of circular aperture uniformly illuminated can also be written in terms of the zero-order Bessel function $J_0 = [\dots]$ [**Wynat 1992**].

$$I(r) = I_{\max} \left| \int_0^1 J_0[(kar)\rho] \rho d\rho \right|^2 \quad (2.40)$$

where ρ = radial coordinate for the exit pupil. It is usually normalized.

The irradiance of diffraction pattern of circular aperture having a rotationally symmetric pupil function $(\delta(\rho))$, which is illuminated with a uniform beam, is

$$I(r) = I_{\max} \cdot \left| \int_0^1 \delta(\rho) \cdot J_0[(kar) \cdot \rho] \rho \cdot d\rho \right|^2 \quad (2.41)$$

For spherical aberration, the rotationally symmetric pupil function is

$$\delta(\rho) = \exp(i \frac{2\pi}{\lambda} W_{040} \rho^4) \quad (2.42)$$

where W_{040} = wavefront aberration coefficient for spherical aberration, its equal $\frac{1}{8} S_1$

if defocus is included, then [**Wyant 1992**],

$$\delta(\rho) = \exp(i \frac{2\pi}{\lambda} (W_{040} \rho^4 + W_{020} \rho^2)) \quad (2.43)$$

$W_{020} = \pm \lambda / 4$ wavefront aberration coefficient for focus, its first-order properties of the wavefront and is not Seidel aberration.